PORTABLE LOW COST ULTRASOUND IMAGING SYSTEM

A Thesis

by

Mohammad Rahim Sobhani

Submitted to the
Graduate School of Sciences and Engineering
In Partial Fulfillment of the Requirements for
the Degree of

Master of Science

in the
Department of Electrical and Electronics Engineering

Özyeğin University
August 2015

PORTABLE LOW COST ULTRASOUND IMAGING SYSTEM

Approved by:

Associate Professor G. Göksenin Yaralıoğlu, Advisor
Department of Electrical and Electronics Engineering
Özyeğin University

Associate Professor H. Fatih Uğurdağ
Department of Electrical and Electronics Engineering
Özyeğin University

Associate Professor Ayhan Bozkurt
Department of Electrical and Electronics Engineering
Sabancı University

Date Approved: 19th August 2015

To my cute love and wife, Negar Majidi ...

ABSTRACT

The use of ultrasound in medicine has increased in the last decade either in diagnostics or in treatments. Ultrasound is safe and easy to use compared to other imaging methods, such as X-ray imaging. Various probes are used to image different body parts and internal organs. Probes usually employ a transducer array. Typically these transducer arrays have 64, 96 or 128 elements. While in use, each element of the transducer is driven by a dedicated beam former electronics in transmit an receive. A typical ultrasound system costs somewhere between $100K to $250K. Recently, low cost laptop computer based ultrasound systems have been developed to facilitate the common use of ultrasound devices. The cost reduction is achieved by reducing the channel count. However, even these systems are quite expensive, on the orders of $20K (except a few systems). This high cost limited the wide use of these systems.

This thesis aims the design of a mechanically scanned hand-probe for ultrasound imaging with a significantly reduced channel count (2-4 array elements). The operator will scan the organ to be imaged by the motion of his/her hand. The probe will consist of the transducer, inertial sensors and the driver electronics. While the probe is swung on the body of the patient, the movement of the probe in the 3D space will be monitored by inertial sensors. Acceleration and rotation data from the inertial sensor will be converted to location data by the use of a positioning algorithm (Quaternion estimator), and this data will then be used for the construction of the ultrasound image. This approach will significantly simplify the transducer electronics and, hence, will reduce the system cost.

ÖZETÇE

Tıpta ultrason kullanımı teşhis ve tedavi için son on yılda artmıştır. Ultrason X-ışını görüntüleme gibi görüntüleme yöntemlerine nazaran kullanımı daha kolay ve güvenlidir. Çeşitli sondalar farklı vücut parçaları ve iç organlarını görüntülemede kullanılır. Sondalar genellikle transdüser dizisi olarak kullanılır. Genelde bu transdüser dizilerinin 64, 96 veya 128 elemanı vardır. Kullanımdayken transdüserin her elemanı gönderme ve alma için atanmış ışın şekillendirici elektronik cihazlar tarafından sürülür. Tipik bir ultrason sisteminin $100K ile $250K arasında maliyeti vardır. Son zamanlarda düşük maliyetli dizüstü bilgisayar tabanlı ultrason sistemleri, ultrason cihazlarının ortak kullanımını kolaylaştırmak için geliştirilmiştir. Maliyet azaltma ise kanal sayısını azaltarak elde edilebilir. Ancak $20K civarındaki birkaç sistem hariç bu sistemler bile oldukça pahalıdır. Bu yüksek maliyet bu sistemlerin yaygın kullanımını sınırlamaktadır.

Bu tezde bir ölçüde azaltılmış kanal sayısı (2-4 dizi elemanları) ile ultrason görüntülemesi için mekanik taranan el sonda tasarımı amaçlanmaktadır. Organı tarayan operatör elinin hareketi sayesinde görüntüleri elde edebilecektir. Sonda transdüser, atalet sensörleri ve sürücü elektroniğinden oluşacaktır. Sonda hastanın vücudunda dolaştırılırken, test çubuğunun hareketi 3 boyutlu uzayda atalet sensörleri tarafından izlenecektir. Atalet sensöründen alınan hızlanma ve rotasyon verileri, konumlandırma algoritması (Quaternion tahmincisi) kullanılmasıyla konum verilerine dönüştürülür ve bu veriler daha sonra ultrason görüntüsünün yapımı için kullanılır. Bu yaklaşım, önemli ölçüde transdüser elektroniğini basitleştirecek ve bu nedenle sistem maliyeti azalacaktır.

ACKNOWLEDGEMENTS

I have had the advantage and honor of working with Prof. G. Göksenin Yaralıoğlu, my research advisor for almost the last two years. I have learned so much from his technical knowledge, his research experiences and his kindness. I thank him for patiently listening to me and sharing his opinions.

I would like to thank Assoc. Prof. A. Sanlı Ergün (TÖBB University, Ankara) and Assoc. Prof. Ayhan Bozkurt (SABANCI University, Istanbul) those who are brilliant members of this joint project and Assoc. Prof. H. Fatih Uğurdağ who found free time in his busy schedule to be member of committee. I appreciate TTO (Technology Transfer Office) of ÖZYEĞİN University and TÜBİTAK (the scientific and technological research council of Turkey) for financial support.

Great thanks to my old friend and colleague, Seyedfakhreddin Nabavi. Although the time is coming to miss him, but our friendship is forever; I wish him all the best and success in his future life and career.

Also specially thanks to my wife, Negar Majidi, our parents, relatives and all those who helped and supported me during the this period of my life and education.

Moreover, I wish to all of my friends every thing that they want to have and achieve.

TABLE OF CONTENTS

LIST OF TABLES

LIST OF FIGURES

CHAPTER I

INTRODUCTION

Ultrasound was first applied as a medical diagnostic tool in 1940 while a piezoelectric transducer was used to generate acoustic waves in human body, as well as to collect reflected waves versus time [1]. The amplitudes of reflected acoustic waves were collected and stored versus time. This technique of scanning based on amplitude of reflected data, later called "A-scan mode". Nowadays usually ultrasound probes employ a transducer arrays which usually have 64, 96 or 128 elements [2]. Each element of the transducer is driven by a dedicated beam former electronics both in transmit and receive [3].

To create an ultrasound image, all reflected data (A-scan mode) are needed as well as their corresponding location [4]. The beam former is responsible to change direction (and focus point) of ultrasound waves as well as adding ability to probe and system to get 2D and 3D images, without mechanical scanning. However, due to high channel count (large number of transducer elements) and large amount of data that needs to be processed, ultrasonic imaging systems are quite expensive. Although a real time ultrasound probe was developed in 1978 while a small motor inside a probe was sweeping single transducer [5], but it brought its own problems such as extra electrical and mechanical units for driving motor, low precision and motion artifacts.

To address these limitations, we propose using a mechanically scanned hand-held probe for ultrasound imaging with a significantly reduced channel count (2-4 array elements). The mechanical scanning will be achieved by the hand movement of the operator [6-9]. While the probe is swung on the body of the patient, the movement of the probe in the 3D space will be monitored by inertial sensors. Acceleration and

rotation data from the inertial sensor will be converted to location data by use of a 3D positioning algorithm and these data will then be used for construction of the ultrasound image. This approach will significantly simplify the transducer electronics and hence, will reduce the system cost. For further cost reduction the transducer should also manufacture using a low cost manufacturing method. To improve the focusing ability and the penetration depth of the transducer, we are planning to use an annular array. CMUTs are ideal candidates for this work [10,11]. Using annular array for the probe, will give us ability to fully control the ultrasound beams such as changing focal length and penetration depth, whereas its manufacturing procedure is easy and cheap.

The final system will have some advantages: 3D images of desired tissues can be captured easily by rotating the probe in all directions. Because the probe will use wireless module to transfer data, then It can wirelessly send the images (or raw data) to host computers or android devices which run the required program. More importantly, since the probe is hand-held and portable, it can be used in ambulances in emergency cases where there are internal injuries or emergency situations, in clinics for pre-examination checkups and etc. Moreover, because cost of the system will be reduced by using this method, therefore costs of diagnosis and routine checkups will be dropped.

In the next section of the introduction, basic of ultrasound will be introduced. In next chapter, portable ultrasound machines will be reviewed. In chapter 3 details of our method will be presented as well as results. And finally, chapter 4 will conclude the thesis.

1.1 Basics of Ultrasound Imaging

Ultrasound is an acoustic wave that has frequency upper than 20 KHz or upper than human hear-able frequency range. Ultrasound waves can be produced by using specific speakers (mechanical movements of diaphragm due to current changes inside a permanent magnetic field) or Piezoelectric material (specific ceramic materials which changing the voltage over two side of it changes the ceramic shape and reversely, squeezing the ceramic produces voltage on it) or CMUT technology (two plates of capacitor that usually one of them is fixed and changing voltage between plates produces electrostatic forces and finally movement of plate). Ultrasound transducers usually have ability to transmit and receive ultrasound waves, that is why they some times call ultrasound transceivers. In medical applications as well as most industrial applications, the ultrasound transducer that is used for producing ultrasound is used for collecting or receiving the reflected ultrasound waves too.

Suppose we have a ultrasound transducer that produces ultrasound inside a water as shown in Figure 1. The transducer sends ultrasound waves at specific frequency and small time period then receives the reflected waves. The ultrasound wave travels entire the water container till arriving bottom of it. The reflected waves from the bottom will reach the transducer with small amplitude which is dropped during the traveling inside the water (water has attenuation like all material and human tissues). Therefore the collected waves from transducer should have small amplitude in compare to stimulated signal's amplitude. Also the time between the transmit and receive shows one round trip of ultrasound wave inside the water (not exact traveling time). While one rigid object is put in water, another reflection wave is added between the transmit wave and reflection from bottom. Multiple reflection can be captured by receiver (Echo), because the ultrasound waves will be reflected multiple times between bottom, transducer itself and objects; However, attenuation of water or tissue will vanish the multiple reflections. This type of scanning which is based on

amplitude of reflection waves called A-Scan imaging (or Amplitude Scanning) which is based of the medical ultrasound imaging and almost in industrial imaging systems too.

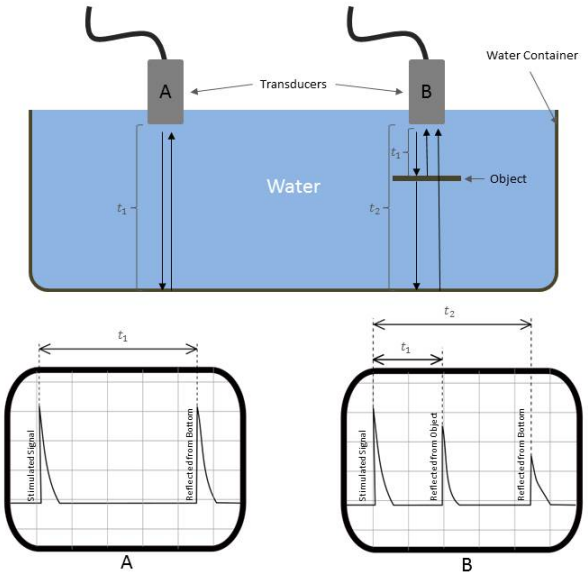

Figure 1: Simple ultrasound reflection of an object in water.

Obviously A just has stimulated and reflection waves from bottom with roughly same amplitude because of low attenuation of water. B transducer gets an extra reflection from object in the water; the amplitude of reflections are dropped while going far from the transducer. also t2 is larger than t1 as is understandable from distances where the object is located between the transducer and bottom of water container.

1.2 Ultrasound Imaging Modes

1.2.1 A-Scan (Amplitude Scanning) mode via single transducer

Amplitude Mode scanning is an old and simplest mode of ultrasound imaging that displays envelope of the echo pulses versus time. It usually uses single transducer in medicine which depends to the application; frequency can be 2-15 MHz. The transducers between 2-5 MHz can be used for brain, cardiac imaging (where the

high penetration is required) and transducers between 5-15 MHz use for ophthalmology (determines the distances between different regions of the eyes) and so forth. Although high frequency bring high axial resolution, but attenuation due to high frequency some times is not matter because ultrasound machines use TGC (Time Gain Compensation) amplifier. we will go to more detail about TGC amplifier later. A simple image of A-Mode is demonstrated in figure 2.

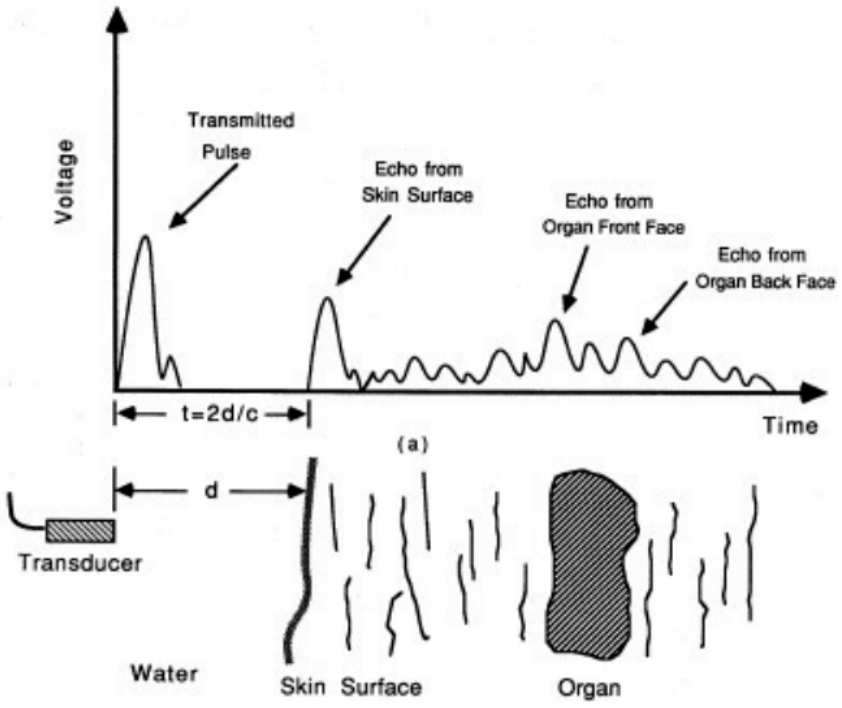

Figure 2: An example of A-Mode scanning

Here Envelope detection is used for Output signal. And water acts as matching layer between body and transducer. The figure is reprinted from Prince and Links text book.

As mentioned before A-Scan mode usually uses single transducer either in industrial or in medical application. Figure 3 shows a cross section of single transducer with some common types of transducers.

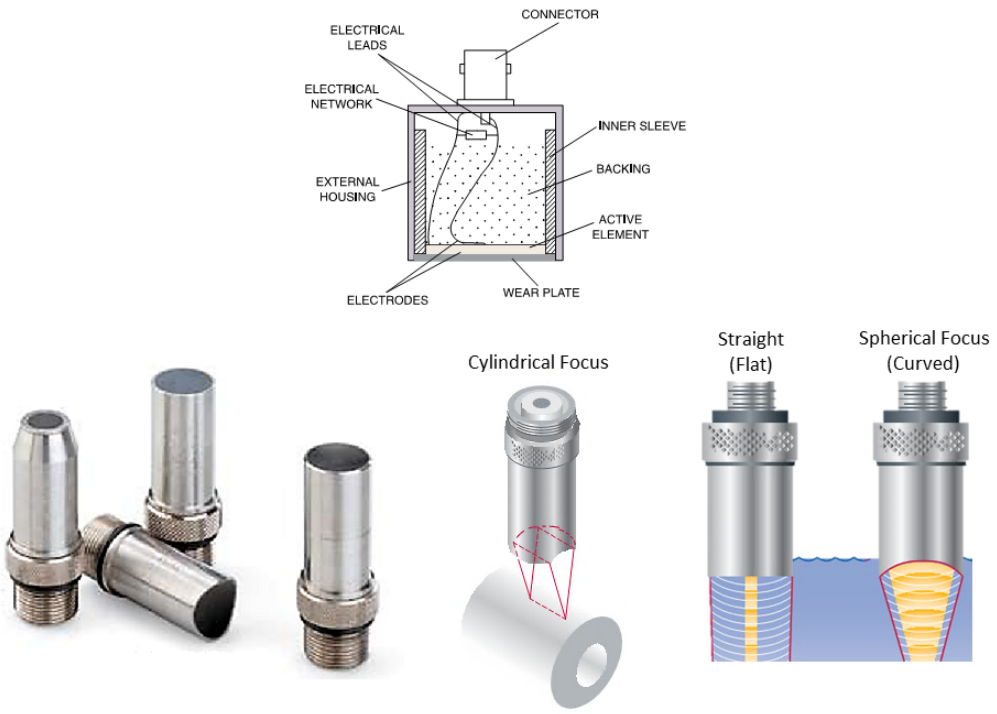

Figure 3: Some kind of single transducers

Depends to the application, suitable transducer can be used either in medical or industrial application. These transducers mostly are built from Piezoelectric material. Reprinted from Olympus application notes.

1.2.2 M-Scan Mode

M-Scan Mode also uses single transducer for imaging. It displays the A-Scan mode signals corresponding for repeated stimulated pulses for a fixed transducer position and puts each gotten A-Scan in separate column of 2D image. It usually uses for movement detection of a part of an organ such as tracking heart's valves movements.

1.2.3 B-Scan Mode

While A-Scan mode displays a line of image form single fixed transducer's reflection; B-Scan mode gets a line of image from different position while a single transducer is

moved or array of transducers is used. B-Scan mode provides a 2D image from body. Most medical ultrasound machines use this method for imaging of organs inside the patient's body. Depends to the ultrasound imaging type and where it used, different type of the ultrasound transducers or Probes should be used. Figure 4 shows some kind of probes that are used for B-Scan mode.

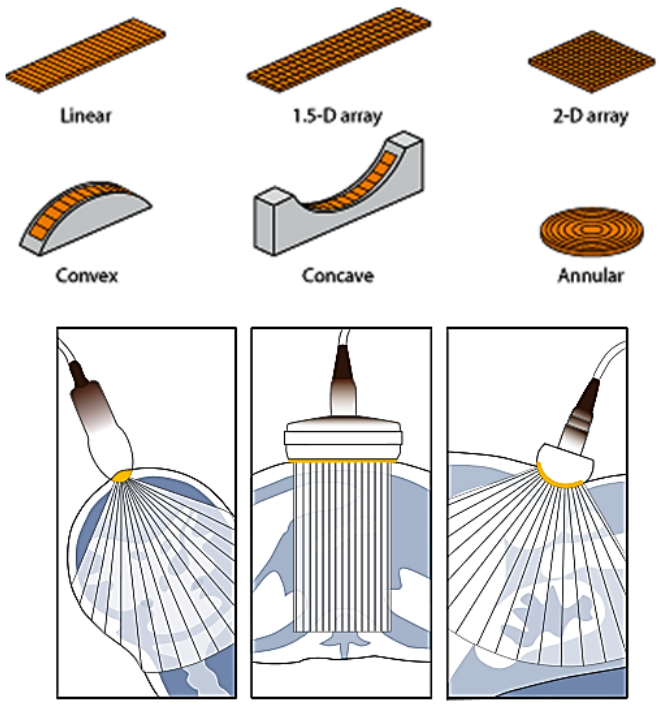

Figure 4: Frequently used medical ultrasound probes

Linear or planar probes mostly are used for Thyroid, Stomach, etc. scanning and Curved ones are used for Heart, Pregnancy and etc. Reprinted from Olympus application notes.

Driving of each single transducer is so important and critical in B-Scan mode and that is the most effective reason that makes ultrasound machines so expensive and bulky. Usually array transducers are built by gathering large number of single tiny transducer beside together. Some times transducer counts reach to more than 100 too. For getting good result and having full control on transducer beams and changing penetration length; usually each transducer uses its own electronic and

beam former. Good imaging can be gotten from an area of organ which ultrasound beams are focused there. For doing focus on all area of an organ, beam former send the stimulated signals to each transducer with delay, so it give a probe ability for focusing. This focusing are changed during the small period to make sure it covers all scanning areas of transducer.

CHAPTER II

PORTABLE ULTRASOUND MACHINES

2.1 Portable ultrasound systems and their capabilities

Because the commercial and advanced ultrasound machines usually are so expensive and bulky, doctors can not benefit them routinely in pre examination procedures. These expensive ultrasound machines are usually used by sonographer not by related specialist doctors, that can complicate diagnosis procedures long and make it expensive too. Figure 5 shows an ultrasound machine that are quite bulky from Siemens company.

Figure 5: An ultrasound machine from Siemens, Acuson x300

The figure demonstrates Acuson x300 from Siemens company. Obviously system is bulky and using that inside ambulances or in emergency situations seems impossible. The figure is reprinted from Siemens web page.

While doctors use stethoscope routinely for hearing sounds of the heart and lungs, then they decide about their functionality. But they usually don't have ability to get an ultrasound image from organ easily without expensive ultrasound machine. Miniaturization of electronic parts could solve some of these problems and could to reduce costs, but not as expected.

Because ultrasound beams are not harmful to human tissue and organs like X ray scanning, but still their equipments are quite expensive for use or even for patients in pre-examination procedure. By reduction cost and size of the ultrasound machines, they can be used almost in all clinics even for simple check up beside stethoscope. These are the reasons that highlight the portable ultrasound imaging systems and their application. The accelerated miniaturization of electronics, especially ASICs (Application Specific Integrated Circuit), made possible to produce portable imaging systems for arrays with full high quality imaging capabilities. Recently low cost laptop computer based ultrasound systems have been developed to facilitate the common use of ultrasound devices. The cost reduction is achieved by reducing the channel count. The aim was to increase the use of ultrasound systems by doctors. However, even these systems are quite expensive, on the orders of $20K (except a few systems).

Most commercial portable ultrasound imaging systems use limited number of the transducer built in array transducer. Thus they don't need more electronic boards and size is decreased. These machines usually have not good resolution as bulky commercial machines have, but still are accepted and enough for clinical pre-examination checkups. Figure 6 shows MobiUS SP1 system from MobiSante company that is a portable ultrasound machine. It has a cable to transfer data to screen and uses array transducer. Also some of its specifications are, image resolution up to 480x480, it is light enough that can be fitted in doctor's packet, it supports 3.5 and 5 MHz for Abdominal scanning, while 7.5 and 12 MHz for vascular and small organs scanning. During the writing this dissertation, the system costs around 7000 US Dollars that it

is really cheap in compare to bulky and stationary ultrasound machines. But still is expensive for in developing countries.

Most portable ultrasound machines have ability to drive different type of transducers and at different range of operation frequency. They usually are used for primary care such as, abdomen, kidneys, thyroid, soft tissues scanning and etc. Also they can be used in emergency medicine such as, pregnancy confirmation, cardiac and chest scanning and etc.

There are some different type of portable ultrasound machines that use 2D array of transducers for getting 3D images of organs, but however the method almost is same as bulky and expensive commercial ultrasound machine that still does not let companies to produce cheap versions with same functionality and so cheap. Same as commercial bulky ultrasound machine they usually use PZT based transducer that are expensive and needs for complex driving and electronic parts.

We will introduce a novel method for portable ultrasound imaging system that will provide an opportunity to produce so cheaper system that gives operator more freedom of ultrasound scanning for getting either lateral or 3D image of an organ.

Figure 6: MobiUS SP1 portable ultrasound system

The figure demonstrates MobiUS SP1 system from MobiSante company. The figure is reprinted from MobiSante web page.

2.2 How our approach reduces cost and size of the ultrasound machine

The most ultrasound probes that are used for imaging have been built by array of transducers. The numbers of transducers depend on the applications and probe types usually are 64, 96, 128 or more. If we assume that each transducer is stimulated separately and reflected data are collected by same transducer when rests of the transducers are off (without beam former); then in this configuration each transducer gets a line of A-Scan or one column of image matrix. Collections of these A-Scans (transducers) beside together create a matrix of an ultrasound image that its dimension is number of the transducer by collected data depth (sampled data for each A-Scan). Although an array with large number of transducers brings high resolution image but it needs to large electronic parts and processors; therefore the system becomes expensive, bulky and stationary. For solving this problem, number of the transducers should be dropped.

Undoubtedly reducing the transducers count will reduce resolution of the image too. The solution that we investigated during this work is; using one transducer which will operate at different 3D positions. In other words, the transducer must be responsible for getting all of the A-Scans data that are required for an organ that we would like to do ultrasound imaging for that. Therefore the transducer has to be moved linearly on the body for lateral scanning (instead of lateral or flat probe) and has to be rotated on the body for curve scanning (instead of curved probe). In this method 3D positions of the probe must be detected frequently and related A-Scan data for each position should be collected. Finally by drawing collections of A-Scans data by respect to their 3D positions at same screen will create an ultrasound image. Figure 7 shows diagram of a system that we would like to aim that. An ultrasound transducer consist of one single transducer (or 2-4 transducers) will connected to inertial sensors and micro controller while 3D position of probe will be calculated periodically as well as getting signals from transducers. Then all data will be transmitted to PC via WiFi connection.

Figure 7: Portable ultrasound probe base 3D motion tracking sensors

The figure demonstrates that 3D tracking sensors are attached to transducer and motion and position of probe is detected and transmitted via WiFi to PC as well as transducer's gotten echo signals.

Because this method will use just a few of transducer, then number of driving

electronic parts such as, pulser, envelope detector, switch and etc. will be reduced. Thus this portable hand held probe will do ultrasound imaging instead of using bulky and so expensive machines in emergency situations.

As mentioned before, the ultrasound imaging based on position tracking will have good resolution if firstly position tracking has good precision and high sampling frequency that will detect each scan lines position enough close to each other; Secondly its transducer should have good focus within operations regions. These types of ultrasound probes some times are named ultrasonic stethoscopes or personal imagers since they allow doctors to look at inside the body at physical examinations and provide rapidly feedback of patient status for further treatment.

Main part of the this project is how to calculate the probe (Transducer) position in 3D. The aim of this project mostly is to detect 3D rotation of the probe, because probe will be used for getting B-Scan mode instead of using curved probes. In first step of this project, we implemented 3D position tracking in C language and used single 5 MHz transducer. Later we added our pulser and another electronic parts. We will go to more detail in following sections.

CHAPTER III

MOTION SENSOR BASED ULTRASOUND IMAGING

In this chapter, our approach for portable ultrasound imaging system will be presented as well as set-up units and final results.

3.1 3D Sensor pack and Microcontroller

After doing some research regarding the 3D position tracking, we find out there are so many methods for tracking and implementation [12,13], but because we want to do all processing in a small processor then the algorithm should be light enough while it has accepted results. Accelerometer, Gyroscope and Magnetometer are required to aim 3D position tracking. Accelerometer has good stationary response, but it gets more noise from shaking or sudden movements. Gyroscope has reverse behavior as accelerometer. Gyroscope has ability to recognize and sense suddenly rotation rate, it is not suitable for stationary purposes, because it gets drift. Also these two inertial sensor can be a good pair for each other to compensate weakness of each other, but combination algorithm can be more complex. Moreover, instead of gyroscope, compass can be used with accelerometer to detect 3D position as well in stationary or slow movements with simple algorithms.

As you know, final probe will be small and hand held, so using large board for it it's not recommended either because of its dimension or because of power consumption. Therefor a single chip that has all these sensors built in, was chosen. MPU9250 from Invensense is used for this project. It has Accelerometer, Gyroscope, Magnetometer (Compass), Temperature sensor and internal biasing and interfacing modules that makes the work so easy. Because the chip is so tiny, then many companies are provided simple and small module that contains this chip and can be used easily on

bread board or soldered board. Figure 8 illustrates a module with MPU9250 and its diagram.

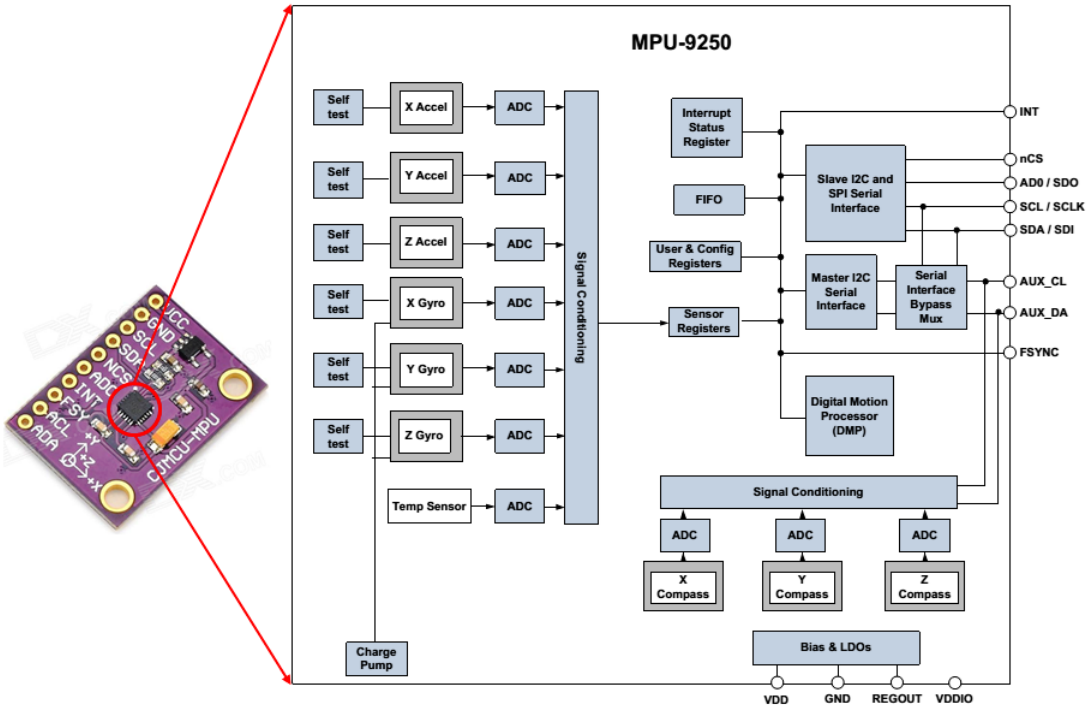

Figure 8: MPU9250 sensor pack

The figure demonstrates MPU9250 chip on a small board and its diagram. The picture is reprinted from MPU9250 datasheet.

One PIC32 microcontroller is used for getting data from MPU9250. Because prototype version of this project has cable connection between sensors and PC, then PIC32 sends raw data to PC through USB cable via HID (human interface device) protocol. According to our research we found out if sampling frequency will be more than 100 Hz for sensor pack, then we will have smooth 3D tracking, so we chose 500 Hz sampling frequency for getting data from sensor pack. The sensor pack has ability to send interrupt to microcontroler if the data are ready, therefore sampling frequency for getting data is adjusted to 500 Hz (each 2 ms) inside a MPU9250. When

the interrupt comes microcontroller reads Acceelerometer's and gyroscope's data via SPI connection, then reads Compass's data via I2C interface which is connected to Auxiliary pins of MPU9250. Figure 9 shows PIC32MX534F064H microcontroller on well provided board from MikroElektronika, known as MINI-32 board and MPU9250 module.

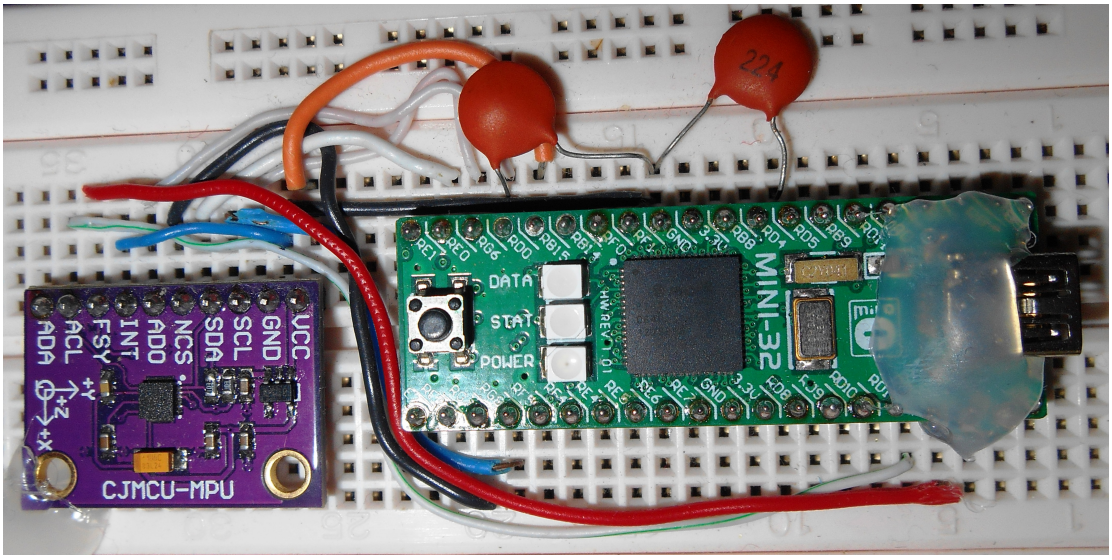

Figure 9: Mini-32 board and MPU9250 module

The figure demonstrates how MPU9250 is connected to Mini-32 board. Mini-32 gets data frequently from MPU9250 and transmits them to PC via USB cable.

Pic32 creates a frame for each gotten data and puts them in it with frame number. Because it uses HID class for transferring data, so maximum frame size for be transmitted is 64Bytes. In other hand some times the program which runs on the PC is totally busy and doesn't let reading function to get transmitted data from microcontroller; finally frame is lost. To prevent that, we used all 64Bytes that can be used for transferring as figure 10 shows.

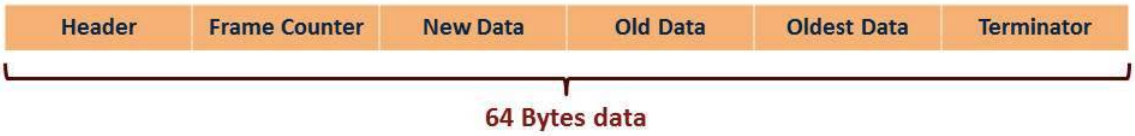

Figure 10: Frame of Sensors pack's data to be sent

The figure demonstrates how the sensors data are filled inside a frame which each frame contains two previous raw data too. it helps to recovery data when a frame is lost.

The old and oldest data are used when one or two frame is lost and PC could not get them, however, it just guarantees to recover two frame lost not more. The sampling frequency of sensors pack can be increased to 1 KHz that USB HID class supports it too and for testing we did 1 KHz sampling too. For prototype version of the system microcontroler just sends the data to PC as interface; it does not do any more processing on the data, but it will do for final version of the system.

3.2 3D Position Tracking

For representing position of rigid object in the 3D space, rotations and linear movements corresponding to the Earth-fixed coordinate are needed while the NED coordinate (North East Down) is used for this work. The ultrasound probe with an ultrasound transducer needs rotations or (and) linear movements detection while its transducers head touches the body, so it has to be able recognize the 6 DOF (degree of freedom) movement in 3D space. For achieve this we need to combine Accelerometer, Gyroscope and Compass sensors data (sensor fusion algorithms). Accelerometers and Gyroscopes are known as inertial sensors since they use property of inertia [14].

The accelerometers sense accelerations due to the earth gravity and linear movement while the gyroscopes sense rate angular velocity around its coordinates. Also the compass sensor senses magnetic field which in absence of extra magnetic fields

due to electrical circuits or permanent magnet, can be used for detecting earth magnetic field while it has accepted stationary response. As mentioned before all these sensors usually are built in a single chip which has digital or analog interface; we used MPU9250 from InvenSense since it has digital interface and adjustable internal sampling frequency source. We assumed coordinate of the sensors x, y, z are towards to the North, East, Down while Roll, Pitch, Yaw are rotations around corresponding coordinates respectively as figure 11 is illustrated. The Roll, Pitch and Yaw are representing the Euler rotation around fixed coordinates. In this method sequence of the rotations are important and unchangeable.

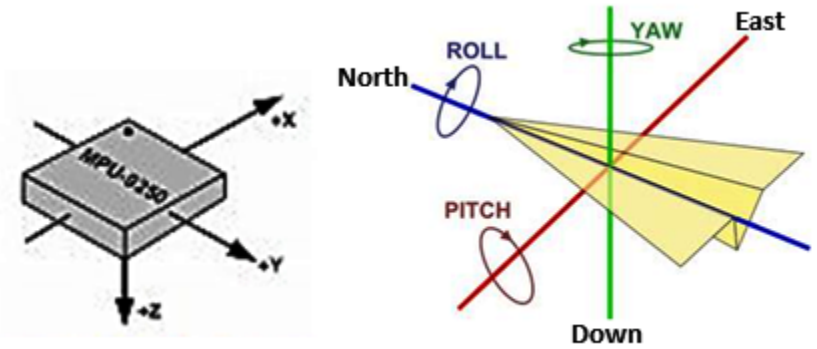

Figure 11: NED Coordinate

The figure demonstrates coordinates of our sensor pack and their related rotations by respect to the NED (North East Down) coordinates.

By using the mentioned architecture, for stationary or slow movement (without shaking) of sensor pack, the accelerometer can detect the Roll and Pitch angles when tilt the frame, but it cannot do it for Yaw. Assume there is a small mass hanged via spring inside the accelerometer. Due to the earth gravity, while accelerometer (sensor pack) is rotated around X or Y coordinates, related angles can be calculated by using simple trigonometric calculation, but accelerometer can not be used for Yaw (rotation around Z axis) detection. Finally for detecting the Yaw rotation Compass sensor is

used because Yaw rotation can be detected easily by calculating the angle between earth magnetic field (which come from north) and x axis of the sensor package.

Because manual scanning of the probe has not more suddenly movement or rotation (roughly stationary movement), thus we used only accelerometer and compass which they have good stationary response. To achieve that, Quaternion estimation algorithm (QUEST) is used [15-17]. The QUEST algorithm is interested to use because representing of rotation by quaternion is simple and it does not need to more processing. Quaternion needs for four parameters to be represented as figure 12 shows. It is a rotation representation method that an unit rotation axis and one degree of rotation are used for it.

$$q_w = \mathrm{Cos}\left(\frac{\theta}{2}\right)$$

$$q_x = V_x \times \mathrm{Sin}\left(\frac{\theta}{2}\right)$$

$$q_y = V_y \times \mathrm{Sin}\left(\frac{\theta}{2}\right)$$

$$q_z = V_z \times \mathrm{Sin}\left(\frac{\theta}{2}\right)$$

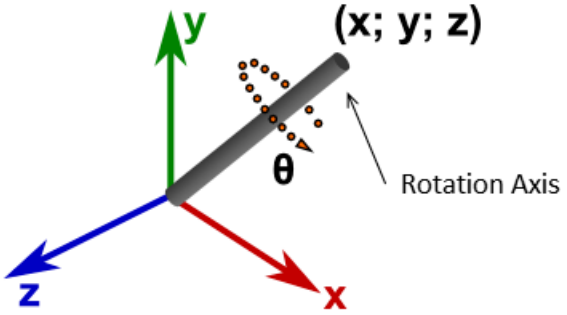

Figure 12: Quaternion rotation

The figure demonstrates how Quaternion rotation can represent rotation of an object in 3D space in all arbitrary directions. The picture partially is reprinted from xojo3d webpage.

Gyroscope can be added to the algorithm when suddenly movement detections are required by using Kalman or Complementary filter [18]. Compass and Accelerometer raw data should pass from low pass filter. The main reason for using LPF is sensitivity of accelerometer to shake and sensitivity of compass to interface wires magnetic field. Figure 13 shows diagram of the Quest algorithm and figure 14 shows how a Gyroscope

can be added to the algorithm to bring high precision 3D detection for suddenly probe movements. We did not use Complementary of Kalman filter for this work, later it will be added too. In this section we will not write any more equation and formula for QUEST algorithm to avoid being complex and confusing. We added simplest QUEST algorithm's C code in Appendix section that was written for this project and still we use it.

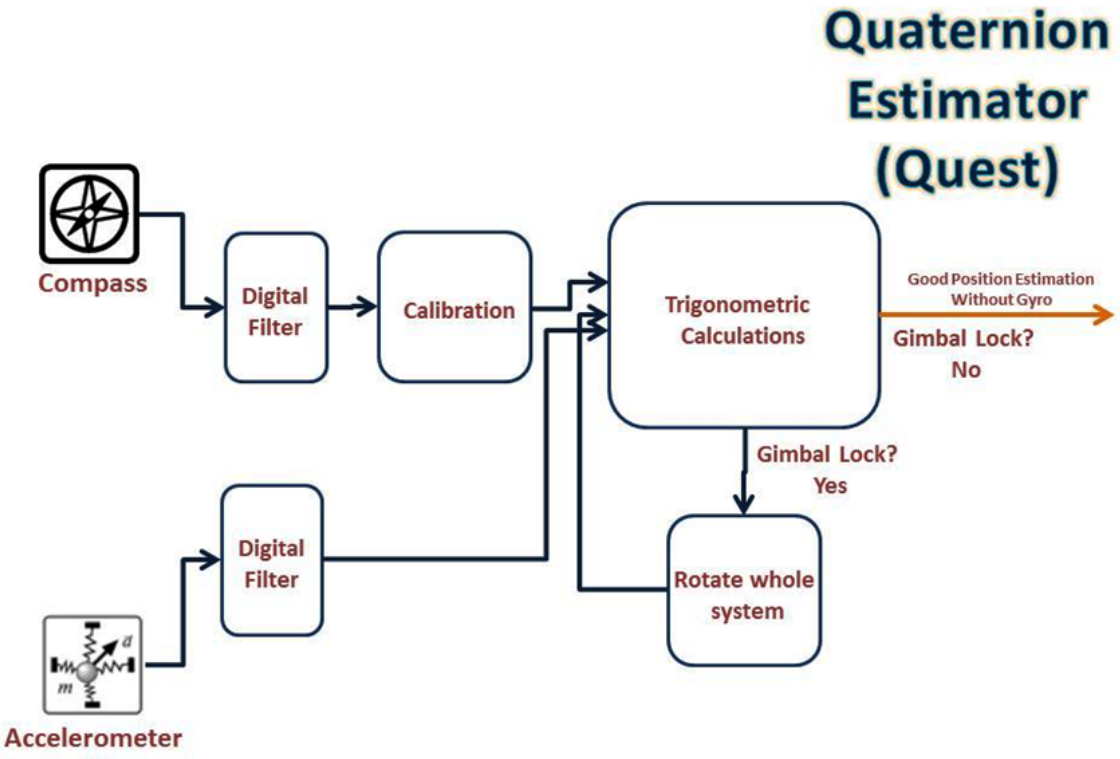

Figure 13: Quaternion estimator diagram (QUEST)

The figure demonstrates a simple diagram of QUEST algorithm. To avoid Gimbal Lock, algorithm has a threshold value that does not let it to be occurred.

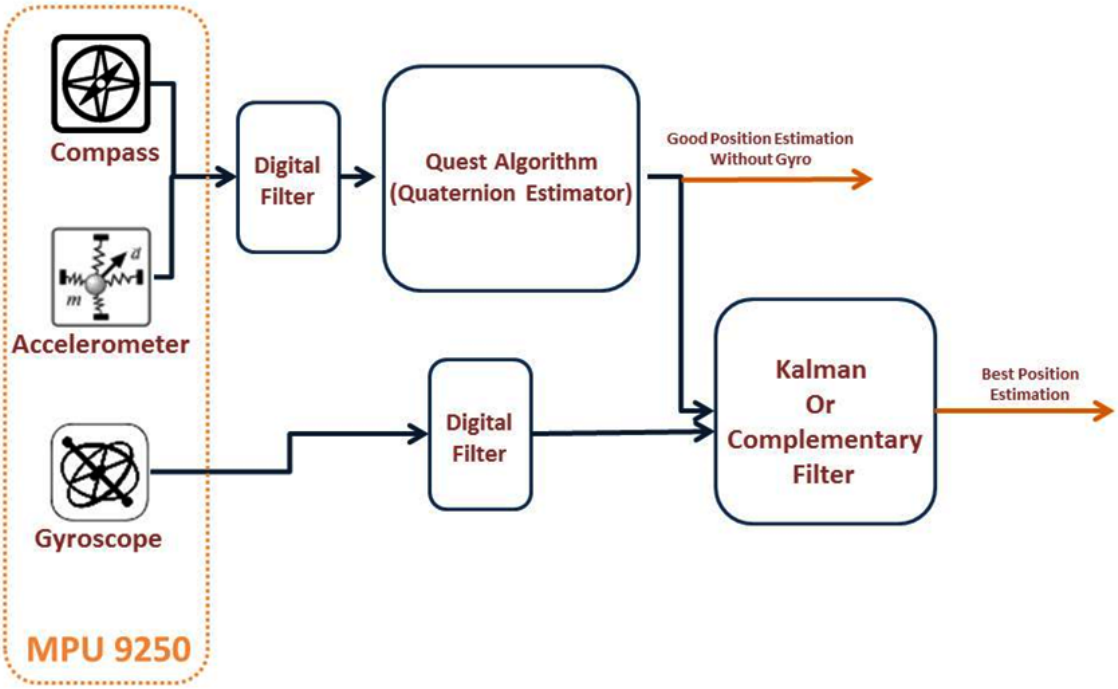

Figure 14: QUEST and Complementary filter

The figure demonstrates how output of the QUEST algorithm can be used and combined with a Gyroscope sensor. This method will able probe and algorithm to sense and recognize shaking and suddenly movements too, however it does not needed for normal application and with just using QUEST algorithm we can aim same performance with low computation load on processor.

3.2.1 QUEST

Here some important equations of QUEST (Quaternion Estimator) algorithm will be presented. As mentioned before, the unit Quaternion rotation can be presented just by four parameters as equation 1 describes that. if β is rotation angle in 3D and u is unit vector, then unit Quaternion's variables can be calculated by equations number 2.

$$
\begin{aligned}
q &= (q_0, q_1, q_2, q_3) \\
q_0^2 + q_1^2 + q_2^2 + q_3^2 &= 1
\end{aligned}
\tag{1}
$$

$$
\begin{aligned}
q_0 &= cos(\frac{\beta}{2}) \\
q_1 &= u_1 sin(\frac{\beta}{2}) \\
q_2 &= u_2 sin(\frac{\beta}{2}) \\
q_3 &= u_3 sin(\frac{\beta}{2})
\end{aligned}
\tag{2}
$$

if sensor pack is stationary or moves slowly, then amplitude of acceleration that is read from 3-axis is one g (gravity of earth). While system has slow movement, then amplitude of 3-axis becomes more or less than one g, normalized value for each axis can be calculated and used. Suppose $\hat{a_x}$, $\hat{a_y}$ and $\hat{a_z}$ are normalized acceleration for each axis, then θ (rotation around y axis, Pitch) can be extracted from equation 3.

$$
\begin{aligned}
sin\theta &= \hat{a_x} \\
cos\theta &= \sqrt{1 - \sin^2\theta}
\end{aligned}
\tag{3}
$$

Because unit quaternion uses half degree of trigonometric equations, then quaternion for Pitch (q_p) comes from equations 4.

$$
\begin{aligned}
sin\frac{\theta}{2} &= sign(sin\theta)\sqrt{\frac{(1 - cos\theta)}{2}} \\
cos\frac{\theta}{2} &= \sqrt{\frac{(1 + cos\theta)}{2}} \\
q_p &= cos\frac{\theta}{2}(1, 0, 0, 0) + sin\frac{\theta}{2}(0, 0, 1, 0)
\end{aligned}
\tag{4}
$$

With same method, Roll (rotation around x axis, ϕ) and its quaternion (q_r) can be calculated as equations 5 show. Here is where the Gimbal lock ($\theta = 90$) makes the

system undefined.

$$
\begin{aligned}
sin\phi &= -\frac{\hat{a_y}}{cos\theta} \\
cos\phi &= -\frac{\hat{a_z}}{cos\theta} \\
sin\frac{\phi}{2} &= sign(sin\phi)\sqrt{\frac{(1-cos\phi)}{2}} \\
cos\frac{\phi}{2} &= \sqrt{\frac{(1+cos\phi)}{2}} \\
q_r &= cos\frac{\phi}{2}(1,0,0,0) + sin\frac{\phi}{2}(0,1,0,0)
\end{aligned}
\tag{5}
$$

As mentioned before, Yaw can not be calculated from accelerometer data. For this project we used Compass data to recognize ψ (rotation around z-axis, Yaw). First, normalized body magnetic field (b_m) is read from compass sensor, and is rotated by respect to the Roll and Pitch rotation. The result is Earth Magnetic field (e_m). Because earth magnetic field is different for each location, then we found magnetic field where the Roll and Pitch angles were zero (it was our calculation for NED system). The magnetic fields that we got from North (x-axis, N_x) and East (y-axis, N_y) are -0.28735 and -0.95783, respectively. Equations 6 show how Yaw (ψ) and its quaternion (q_y) can be calculated.

$$
\begin{aligned}
b_m &= (0, b_{m_x}, b_{m_y}, b_{m_z}) \\
e_m &= q_p q_r b_m q_r^{-1} q_p^{-1} \\
M_x &= \frac{e_{m_x}}{\sqrt{e_{m_x}^2 + e_{m_y}^2}} \\
M_y &= \frac{e_{m_y}}{\sqrt{e_{m_x}^2 + e_{m_y}^2}}
\end{aligned}
$$

$$
\begin{aligned}
cos\psi &= M_x N_x + M_y N_y \\
sin\psi &= -M_y N_x + M_x N_y \\
sin\frac{\psi}{2} &= sign(sin\psi)\sqrt{\frac{(1-cos\psi)}{2}} \\
cos\frac{\psi}{2} &= \sqrt{\frac{(1+cos\psi)}{2}} \\
q_y &= cos\frac{\psi}{2}(1,0,0,0) + sin\frac{\psi}{2}(0,0,0,1)
\end{aligned}
\tag{6}
$$

Finally, while there is no any Gimbal lock problem, final quaternion rotation can be extracted by using equation 7.

$$
q = q_y q_p q_r \tag{7}
$$

Implementations of these formulas in c programming language, are represented in appendix. Before applying these implementation, data should be passed through digital filters to make sure all noises and high frequency components are vanished.

3.2.2 Gimbal Lock

Most 3D tracking algorithms that use trigonometric calculation for detecting rotation angles, have singularity limitation that is called Gimbal Lock. According to the frame that we used for this project (NED), Gimbal lock occurs when pitch (rotation around Y axis) reaches to 90 degrees. Somewhere, inside the calculation there is a fraction that denominator of that is cos(pitch). In Gimbal lock mode, system looses one degree of freedom.

The QUEST algorithm prevents system to reach Gimbal lock. It has a threshold for pitch degree, if value exceeds the threshold value, then algorithm rotates whole system to be enough far from threshold. When all calculations are done, algorithm rotates whole system again, but this time in reverse axis that was rotated before. This method will preserve system from Gimbal lock.

We assumed that the threshold value is 0.1. Then, when $cos\theta \leq 0.1$, algorithm rotates normalized $\hat{a}$ and b_m according to the offset quaternion α. We assumed $\alpha = 20$ degrees. After getting offset of $\hat{a}$ and b_m ($\hat{a}_{offset}$ and $b_{m_{offset}}$) as equations 8 show.

$$\begin{aligned} q_\alpha &= cos\frac{\alpha}{2}(1,0,0,0) + sin\frac{\alpha}{2}(0,0,1,0) \\ \hat{a}_{offset} &= q_\alpha \hat{a} q_\alpha^{-1} \\ b_{m_{offset}} &= q_\alpha b_m q_\alpha^{-1} \end{aligned} \tag{8}$$

Other calculation are done as mentioned in QUEST subsection; this time, by using $\hat{a}_{offset}$ and $b_{m_{offset}}$ instead of original ones. Therefore, the gotten quaternion by using offset values (q_{alt}) must be returned back to original one as equation 9 shows.

$$q = q_{alt} q_\alpha \tag{9}$$

3.2.3 Digital LPF

Accelerometers are so sensitive for shaking, while has good stationary response. In other hand, Compasses are so sensitive for magnetic field that surrounded cables produce. Researches show human body movement can be tracked by getting below 5 Hz data. It is enough to detect probe movement with lowest noise and accepted resolution.

To aim that, we used FIR (Finite Impulse Response) 150th order Low Pass Filter. This filter is designed by MATLAB filter design tool and choosing hamming option. The implementation method is First Direct mode as figure 15 shows it, here b's are coefficients of impulse response.

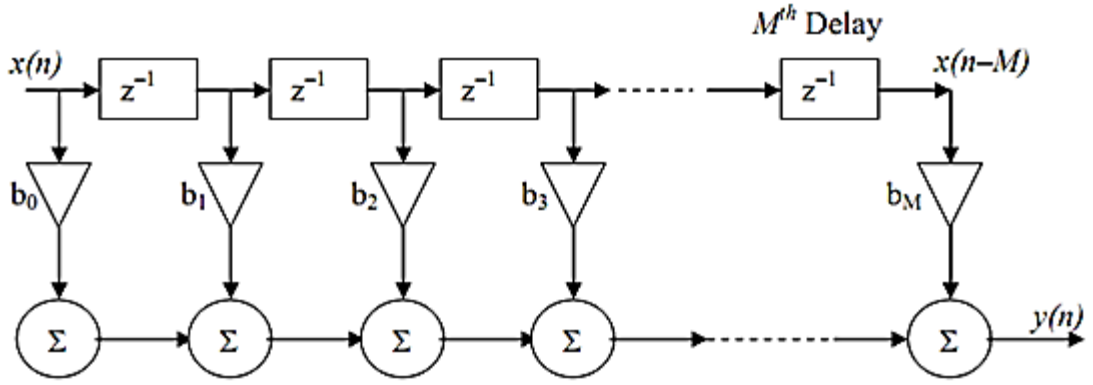

Figure 15: First Direct mode structure for FIR implementation

The figure demonstrates how FIR filter can be implemented by first direct mode structure by knowing discrete impulse response.

The frequency response of this filter with 5 Hz cutoff frequency while discrete signals are sampled at 500 Hz frequency, is shown in figure 16.

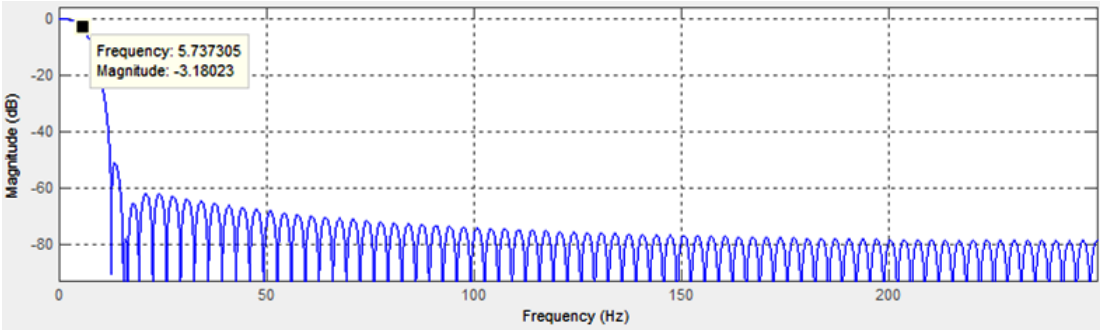

Figure 16: Frequency response of LPF, 5 Hz cutoff @ 3dB

The figure demonstrates frequency response of FIR LPF in 150th order. This filter is used to filter raw data of accelerometer and compass sensor to smooth movement and prevent shaking and vibration.

This filter is implemented to both Accelerometer and sensor data. It is noticeable that MPU9250 it has built in digital LPF, but it's cutoff frequency is not as we proposed. Moreover, MPU9250 just applies LPF to accelerometer that has 20 Hz

cutoff frequency and delays signals for 20 ms. For compass sensor there is no built in LPF, also its initial sampling frequency is 100 Hz while MPU9250, over samples it to 500 Hz.

There is no any guarantee for keeping head of the probe constant on the body or skin during the rotation therefor small linear movement can be occurred. Also for lateral scanning detecting linear movement of the probe is so important. Linear acceleration data can be extracted from the accelerometer data after removing the gravity data. To achieve this, a normal gravity vector (toward the z direction) is rotated according to the QUEST algorithm and result is subtracted from accelerometer raw data. The calculated linear acceleration before integration should pass through a high pass filter to avoid drift. Getting second integration of linear acceleration data gives new coordinator position (translation movement). Figure 17 illustrates the diagram of this algorithm for detection linear movement. Although the code is written and ready for use, but still it has draft and we decided to use another method for detecting the linear movement.

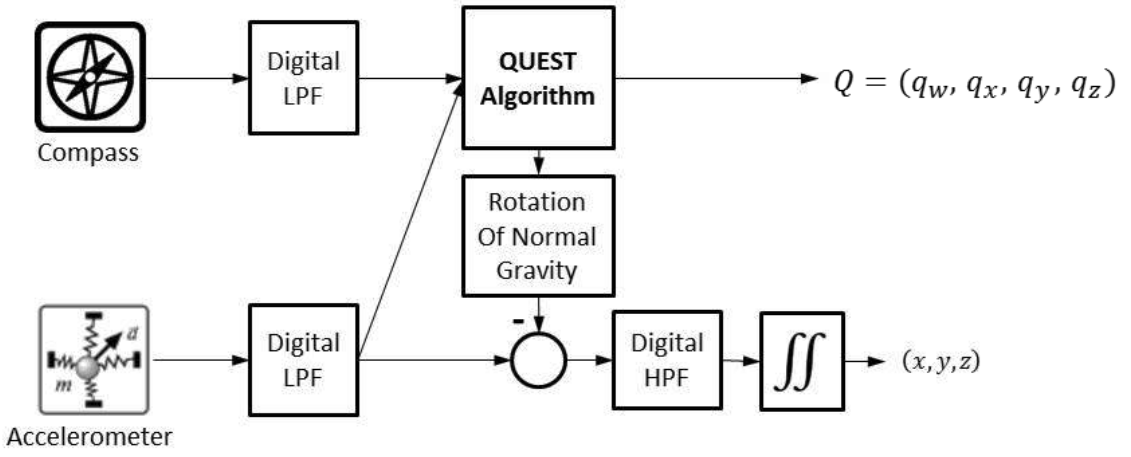

Figure 17: QUEST and Linear Movement

The figure demonstrates how linear movement of the sensor package can be calculated. It will have drift and it should be removed.

This section was one of the most important part of the this project and must work very well to get best result. During writing this dissertation there are some motion detection processors and even modules, but they are quite expensive and does not give more samples in proposed rate (more than 500 Hz). But we still looking for good solution to this part of the project that has examined and high accurate while is cheap and tiny enough to be implemented inside a hand held probe.

3.3 GUI (Graphical User Interface) based on OpenGL

As mentioned before, OpenGL API (Application Programming Interface) is used for graphical processing and environment; because OpenGL is cross platform in compared to DirectX. Final work will be implemented on a system inside a hand held probe which should have ability for do all the necessary processing. Then, OpenGL based codes have ability to be executed on the most laptops, tablets, smart phones and Linux based microprocessors with built in GPU (Graphical Processing Unit). GLFW API (also cross platform) is chosen for creating a window on operation system while loads the OpenGL concepts and makes two way interface between user and OpenGL. For getting good and understandable graphical output, a 3D model of the probe is designed via BLENDER and loaded in OpenGL.

The executed code on laptop reads sensors and ultrasound data via USB frequently as described earlier. After calculating 3D position variables, final results convey to OpenGL as well as related A-Scan (Amplitude Scan) ultrasound data for that 3D position. OpenGL does rotation and translation of whole the system due to the Quaternion and new coordinate variables, then puts 2500 (or 1024) ultrasound data samples as pixels on calculated A-Scan line. It does this loop for predefined number of the lines beside together. figure 18 shows a simple output of the GUI.

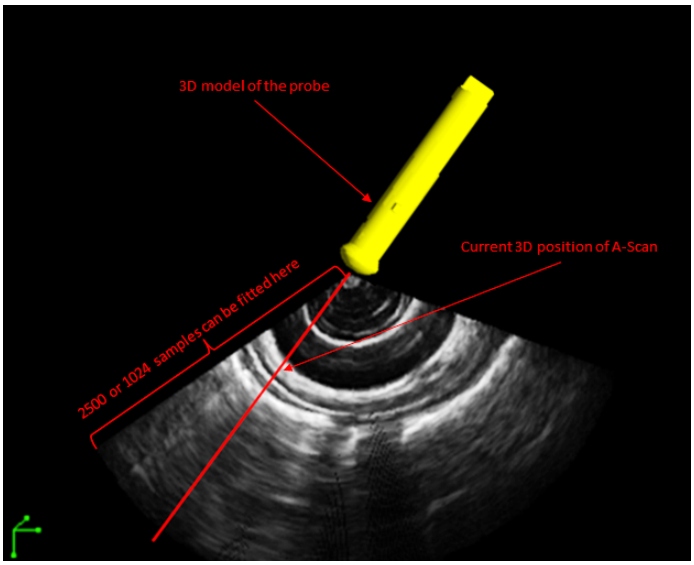

Figure 18: Simple graphical output based on OpenGL

The figure demonstrates how the collection of the A-Scan will be placed beside together to form an ultrasound image.

Final result is collection of A-Scan ultrasound data beside each other corresponding to their 3D positions. Brightness and Time Gain Control adjustments are provided inside the program which make system fully functionality. Also hot keys are defined for program which gives operator fully controlling the see side of the collected data as well as contrast adjustment, stop and so forth. Therefore if a scan is collected in a direction which is perpendicular to the screen and it is not possible to see it clearly, then rotation of see side will solve the problem. Also this feature gives operator to take 3D image of an organ. It is noticeable that golden probe in the image shows the probe shape that gives to operator a real time feedback about rotation and translation of probe. On the laptop that we ran the program, minimum FPS rate (frame per second) was around 10; it depends to GPU performance and number of the lines that are used for creating an image.

OpenGL has value for colors between 0 to 1. Depends to the A-scan samples

(either 1000, 2500 or etc.), one small sphere is dedicated. The gray-scale color for each tiny sphere is determined by its reflected amplitude that is stored. The ADC has ability to pass signal between -2.3 to 2.3V. If Envelope detector is used, then voltage will be around 0 to 2.3V. Software uses equation 10 to convert these voltages to gray-scale colors. TGC[x] is software defined time gain compensation that can be changed by operator during the imaging; predefined value is 1 for all elements. The VGA_{Gain} has value between 0 to 1, similarly it can be changed during the imaging by operator too.

$$Gray_{Scale} = \frac{Signal[x] * TGC[x]}{VGA_{Gain}} \tag{10}$$

We used glColor4f command that uses RGBA (Red, Green, Blue, Alpha) for changing color of each sphere as mentioned before. Because gray scale color is needed for an ultrasound image, then RGB values have same value as $Gray_{Scale}$ and Alpha is 1, as equation 11 shows.

$$glColor4f(Gray_{Scale}, Gray_{Scale}, Gray_{Scale}, 1) \tag{11}$$

3.4 High voltage switch and pulser

Because each transducer is connected to main system via one cable, so stimulated signal goes through a cable that echo's signals will come. In other word, a cable for each transducer act as bidirectional communication. For separating stimulated signal from echos, high frequency switches are used.

While a trigger comes from beam former or processor, the switch connects the simulation signal path to transducer and High Voltage Pulser sends high voltage voltage to transducer in very small period. while stimulated signal is sent successfully, switch connect transducer's cable to receiver circuit. Depends to the application this loop continues frequently for each transducer inside a probe. Figure 19 illustrates simple diagram of these switch and pulser.

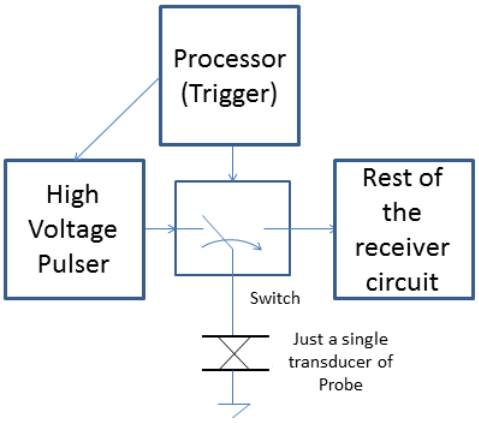

Figure 19: Diagram of Switch and High voltage pulser corresponding for single transducer

3.5 TGC (Time Gain Compensation) amplifier

As you know, sound gets weaker when going far from the source; this is valid for ultrasound waves too because it has same properties like sounds. Each material has special attenuation coefficient for different frequency of ultrasound. When ultrasound beam travels inside a organ or body, it gets weaker when time goes. It means when reflected data are recorded versus time, amplitude of echo drops during the time and brightness of pixels go to be darker. For keeping amplitude of the reflected ultrasound beams same during the time, one amplifier should compensate this attenuation; it calls TGC (Time Gain Compensation) amplifier which its gain increases when the time pasts.

Processor after switching the transducer cable to receiver side, starts to send signal to TGC amplifier for increasing its gain during the time. This controller signal for TGC, depends to the amplifier type can be either digital signal or PWM which should be pass from low pass filter to get suitable analog signal. In some ultrasound machine, there is an option to change the TGC increment rate. It is recommended that use filtering before using TGC amplifier, otherwise all noises will be amplified too.

3.6 Beam forming

For getting good resolution for ultrasound echos, they should be focused on proper location during the scanning. For probes with array of transducers, this focus point has to adjusted by sending stimulated signal for each single transducer with small time delay and maybe with predefined pattern according to the probe model.

Beam former does this job for probe. Figure 20 illustrates a simple beam forming method for focusing the ultrasound beams wherever is expected. Usually processor applies these time delays for each transducer by triggering their switches at the time. With same method and doing some calculation beam steering can be done too. Figure 21 shows how stimulated signals and delays are related to beam focusing of steering.

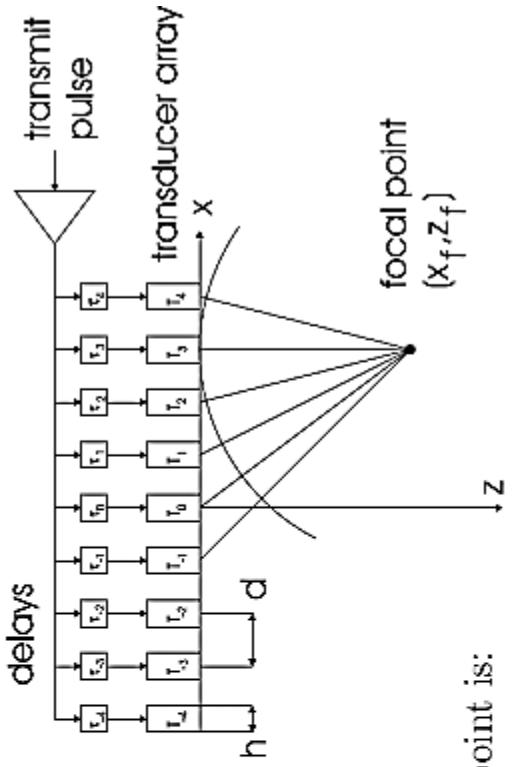

- Focal point at (x_f, z_f)
- T_i is at $(id, 0)$.
- Then range from T_i to focal point is:

$$r_i = \sqrt{(id - x_f)^2 + z_f^2}$$

- Assume T_0 fires at $t = 0$. Then T_i fires at

$$t_i = \frac{r_0 - r_i}{c} = \frac{\sqrt{x_f^2 + z_f^2} - \sqrt{(id - x_f)^2 + z_f^2}}{c}$$

Figure 20: Simple beam former (transmit focusing)

The figure and formulas show how transmit focusing can be achieved by using delay between stimulation of each single transducer. The figure is reprinted from Prince and Links text book.

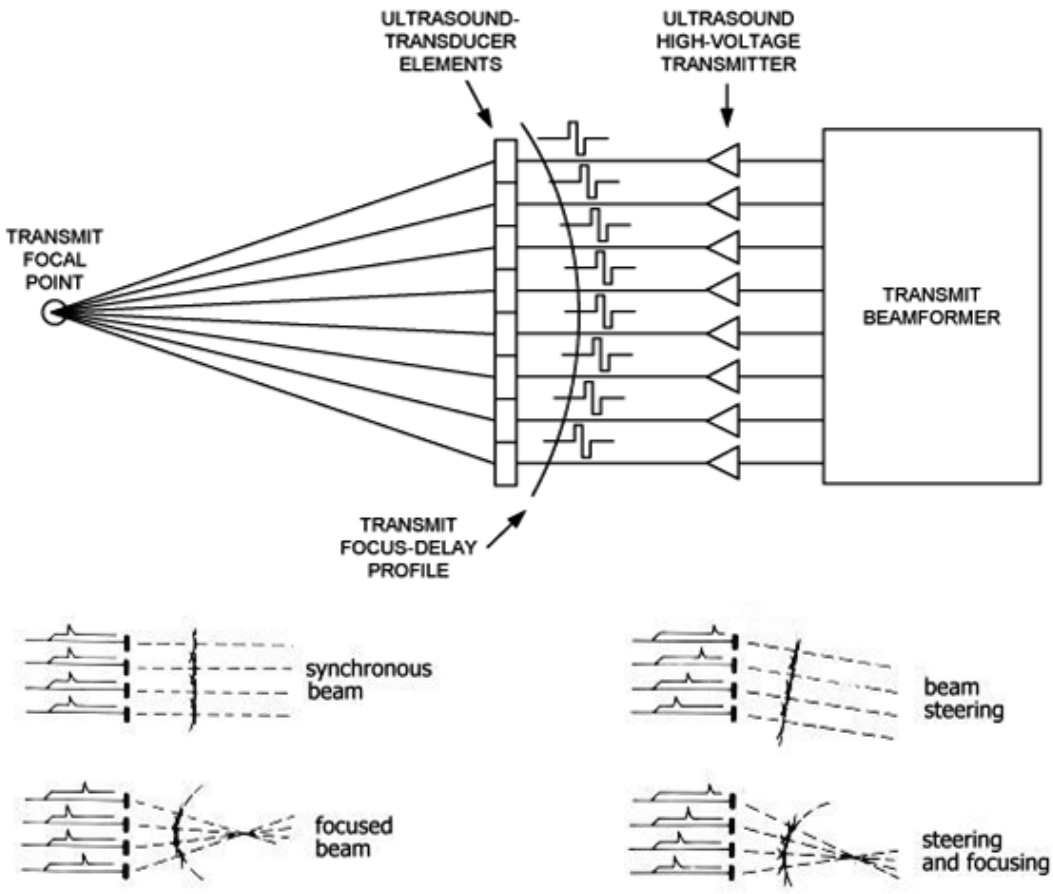

Figure 21: Beam steering and focusing

The figure demonstrates how different type of beam steering and focusing can be achieved by applying proper delay between stimulation of each transducer. The figure is reprinted from Wikipedia web page.

3.7 Envelope detection

In reality the images that have gotten from body have not very large frequency. It means rate of changing on a line of ultrasound images gotten from body (A-Scan) is not very high (frequency of A-Scan from body should be small). Although operation frequency of transducer usually is high but the reflected waves have information of body in low frequency. Similar to the AM (Amplitude Modulation) of a signal,

carrier signal has high frequency rather than the information signal; this is valid for ultrasound reflected signals too. After getting reflected signals, carrier that has high frequency components should be removed from data. the reflected signals should pass through Envelope detector circuit (peak detector or AM demodulator). Using peak detector for reflected data has some advantages, it smooths the reflected signals then smooths the gotten image, also it reduces the sampling frequency that is needed for sampling the signals. A simple circuit of an Envelope detector is shown in figure 22. Because the reflected signals are pretty weak, then using of active Envelope detector is recommended while uses Schottky diode as well as high speed Op Amp. A simple active circuit of Envelope detector is shown in figure 23, the values of capacitor and resistor should be calculated by considering operation frequency of transducer and proper Axial resolution.

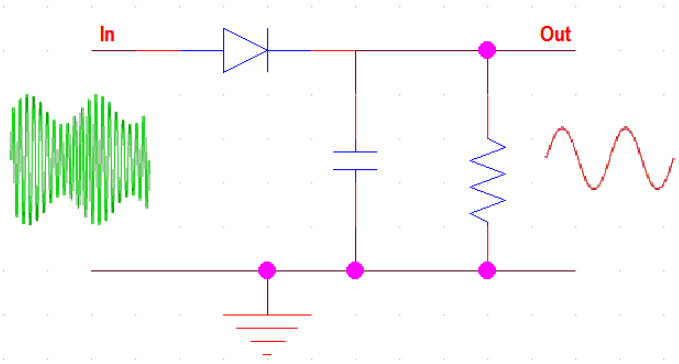

Figure 22: Simple Envelope Detector circuit

Input has both high (carrier) and low (information) frequency, while output just has low (information signals) not carrier.

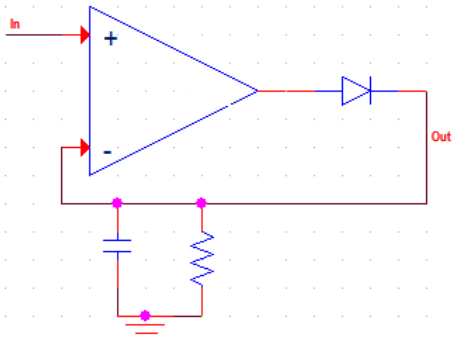

Figure 23: Simple active Envelope Detector circuit

For getting best result, OpAmp should be chosen for high frequency application as well as using Schottky diode with small recovery time.

Suppose ultrasound transducer operates at 5 MHz, then according to the Nyquist law, the sampling frequency should be larger than 10 MHz. If the ADC (analog to digital converter) or microcontroller that does the sampling has limited buffer size, then length of the penetration or collected data varies with sampling frequency; high sampling frequency gives good resolution while will overflow the buffer for small penetration length. For example a transducer operates at 5 MHz and buffer size of the ADC is 1000, therefore getting sampling at 10 MHz takes 0.1 ms while sampling frequency at 20 MHz takes 0.05 ms to overflow the ADC buffer. If the acoustic speed is 1500 meters per second, then first option gives 7.5 cm and second one gives 3.75 cm penetration. Depends to the application, proper length of penetration is desired. For example for pregnancy examination by doing sonography longer penetration is required rather than getting ultrasound image of eyes or skin. thus, using the peak detector is required for reduction of high frequency components (the frequency that transducer operates, in this example is 5 MHz).

To understand it better, a real data is recorded from a transducer which is operated around 3.5 MHz. Configuration of the figure 1, section B is used for data acquisition. The sampling frequency from reflected data was 20 MHz (more than 2

times of transducer's frequency) and ADC buffer got 2500 samples of data. Figure 24 shows the recorded data and it's FFT (fast fourier transform) at 20 MHz sampling frequency without any envelope detector. According to it's FFT, roughly signal has not any more data with frequency higher than 5 MHz; but still it's high and requires high sampling frequency and large buffer for storing the data as mentioned before.

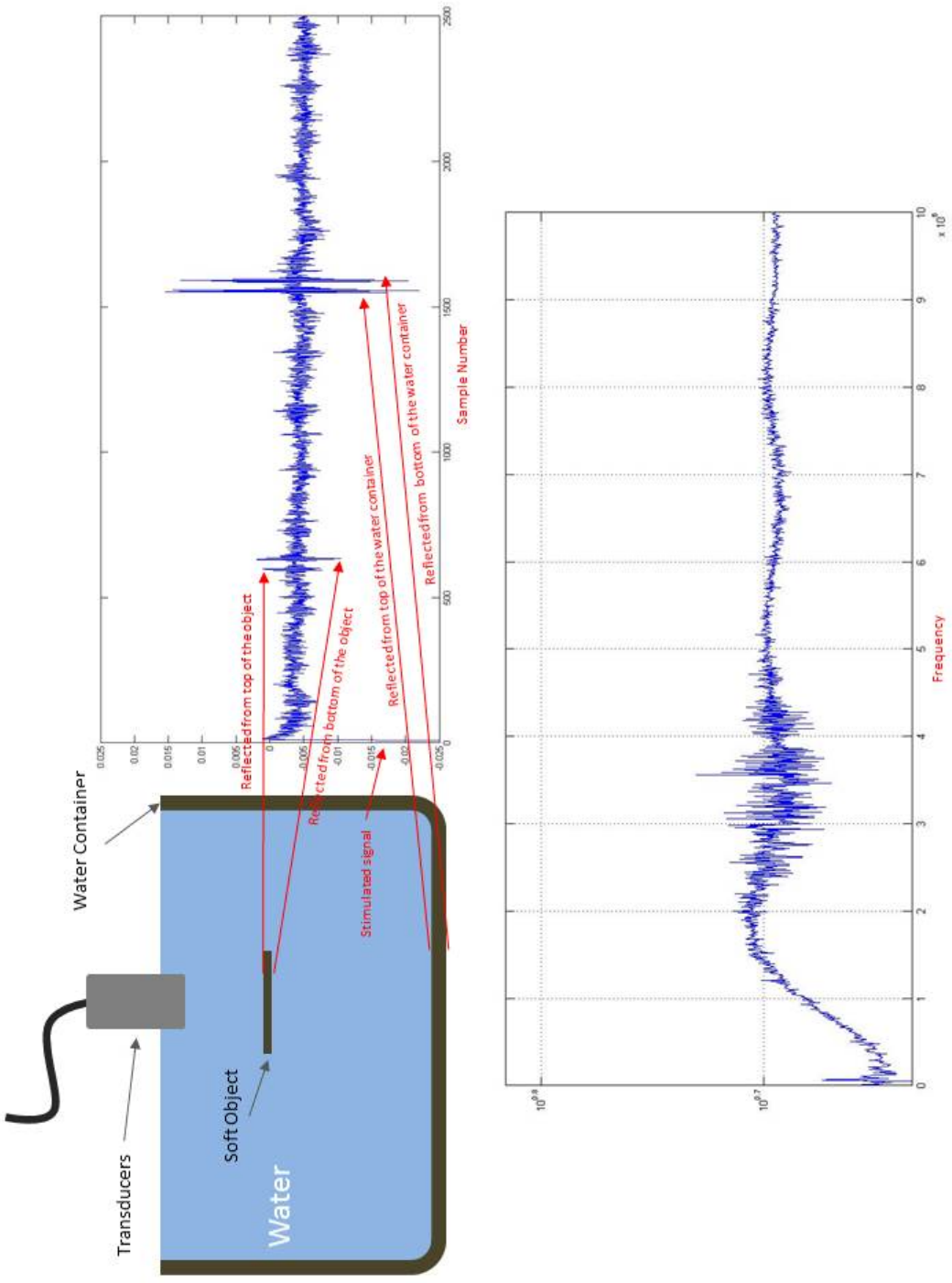

Figure 24: Real recorded data from single 3.5 MHz transducer

As illustrated above; reflected data has 2 local peak points which first one is corresponding to reflection from soft object in water and second one comes from bottom of the water container.

By passing the gotten signal from envelope detector the frequency should be dropped. Because by looking to the signal we can find out that 2 reflection signals from two side of the object has a larger distance rather than the one period of transducer's operating frequency. So as it is mentioned before, by considering accepted axial resolution and frequency of the transducer an Envelope detector can be designed for reducing the frequency of the reflected signal which will bring low sampling frequency and deeper penetration signal record with same buffer size. For understanding it better; the signal of figure 24 is passed through a Envelope detection. The final signal and it's FFT are illustrated in figure 25. It is possible to implement Envelope Detector algorithm inside a processor but still it requires high sampling frequency and large buffer size and it's not recommended.

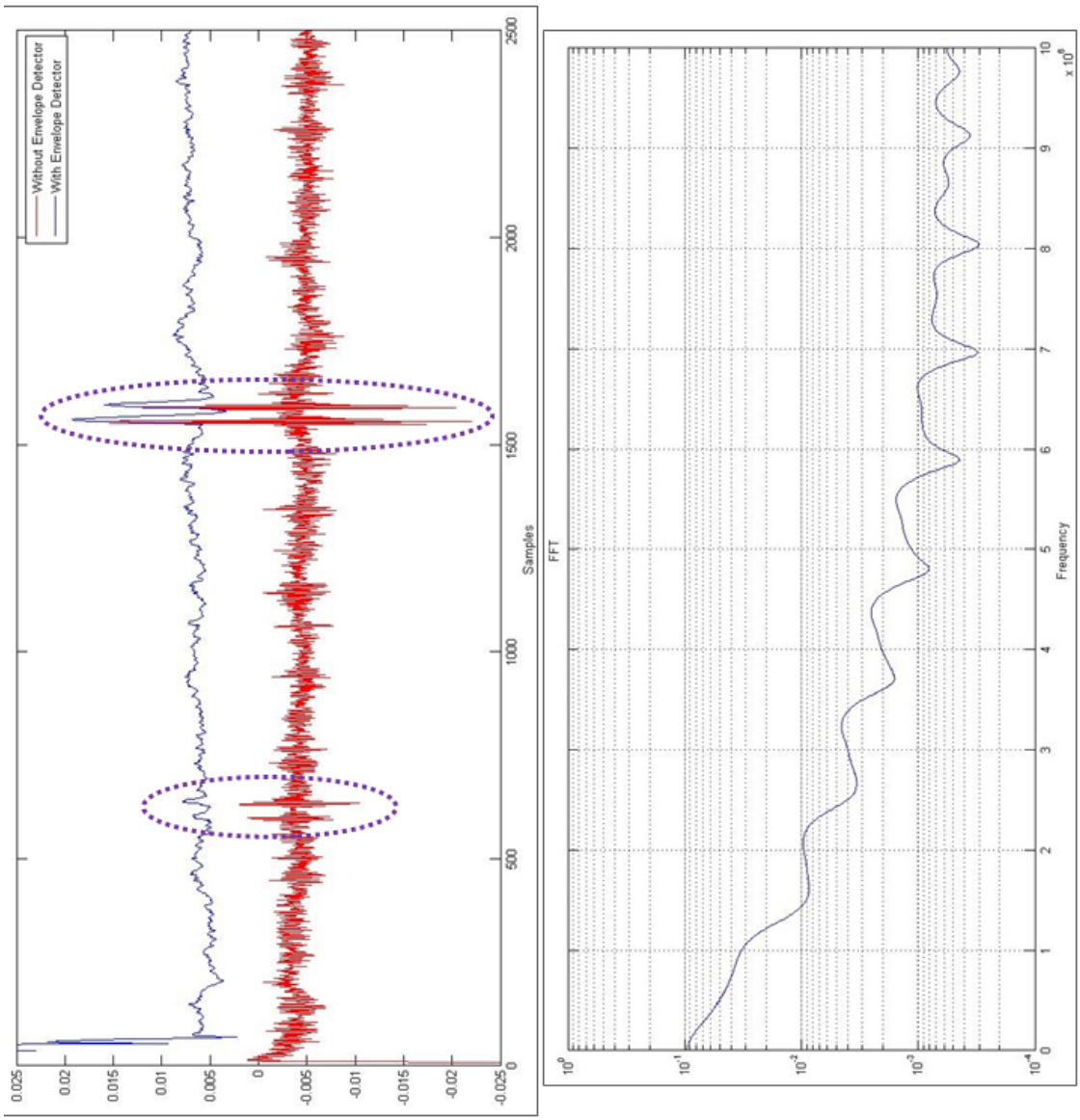

Figure 25: Output of Envelope detector for real 3.5 MHz transducer's data

In compare to FFT of reflected data without Envelope Detector, this one has more low frequency components; it means sampling frequency can be reduced when Envelope Detector is used while the output still has all reflection information from object and bottom of water container.

3.8 ADC (analog to digital converter) board

As you know, analog signal must be digitized to be stored and transferred to PC for further processing. Therefore An ADC module is used for this project that has maximum 40 MHz sampling frequency while uses USB interface to make communication with PC.

An AD9250 IC (from analog device) is connected to CY7C68013A (from Cypress) as figure 26 shows. Both have same clocking source, while a clock comes AD9250 gets a 14 bits sample from analog signal and transfers it to CY7C68013A IC. Cypress IC according to its firmware has 1024 samples FIFO buffer that it is enough for our application. The software that is executed on PC, reads this buffer frequently and according to the stimulated signal (that has large amplitude) recognize the beginning of the samples train and does further processing on it.

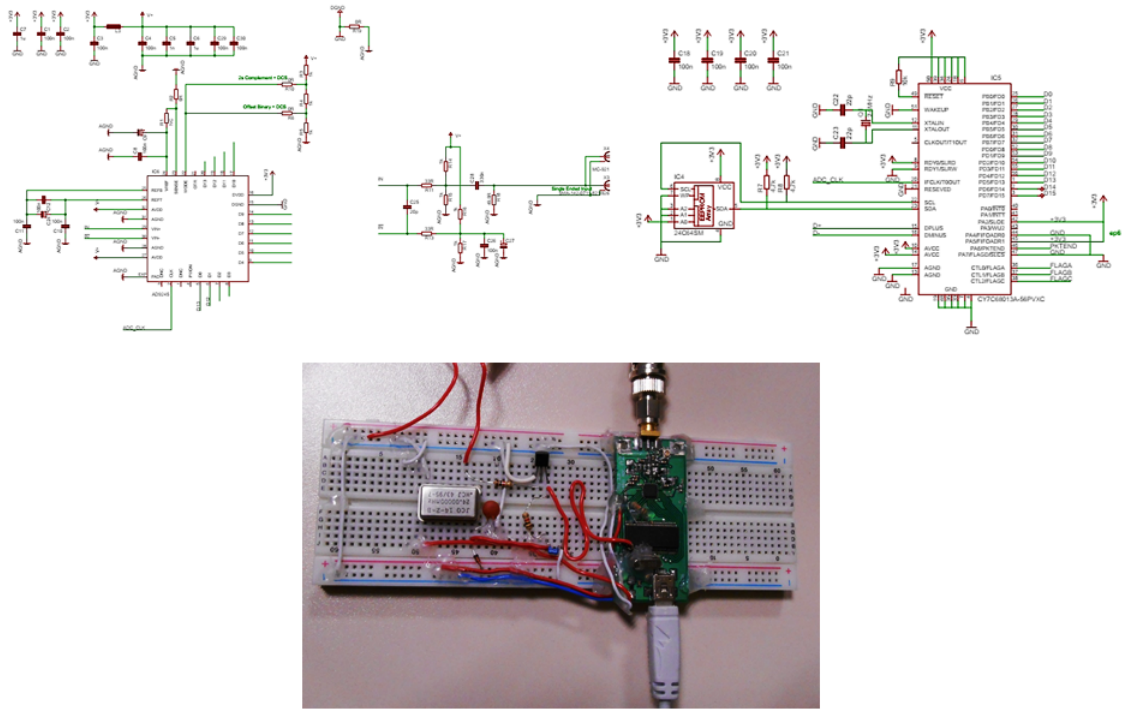

Figure 26: ADC (analog to digital converter) module

The figure demonstrates schematic of the ADC module based on AD9250 and CY7C68013A. The circuit is designed in TOBB university.

The LIBUSB library is used in C language for making communication with ADC module and data acquisition. For first tests we used LIBUSB filter in Windows 8, but OS did not let program to operates and gets data at high rate, because Windows was controlling the module communication. Therefore we use LIBUSB Driver for Cypress in Windows Test mode and we could get data at high rate as possible, however we will optimize the code and maybe firmware to prevent overflow of FIFO buffer and increase data transferring rate. It takes roughly 2 ms to transfer 2500 (2500 * 2 Bytes) Samples to PC through USB cable; Still is good and accepted for us.

3.9 Block diagram of executed software on host laptop

Figure 27 show very simplified block diagram of main code that was executed on host pc. Certainly it has many other sub functions and block diagram, but still this figure give an idea that how programming is done. Renewing the graphic output gets a little bit long time, but that is accepted. Because it does many rotation and translation based on OpenGL and still its performance is good and enough.

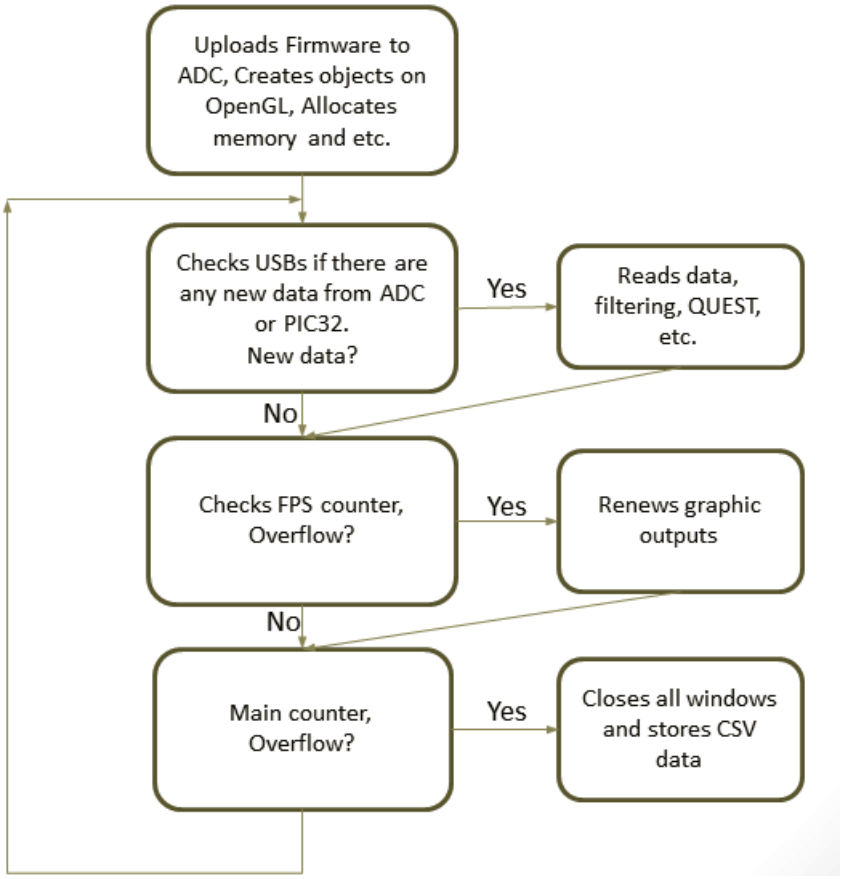

Figure 27: Block diagram of main code executed on host pc

The figure demonstrates how program does its duties.

3.10 First set-up unit with single 5 MHz Piezoelectric transducer

Figure 28 illustrates diagram of our first set-up configuration with single 5 MHz transducer. Because later we will use Wireless communication for transferring data between probe and Host (PC, Laptop, Tablet and etc.), then wireless connection also is used for this testing set-up via WiFi USB dongle.

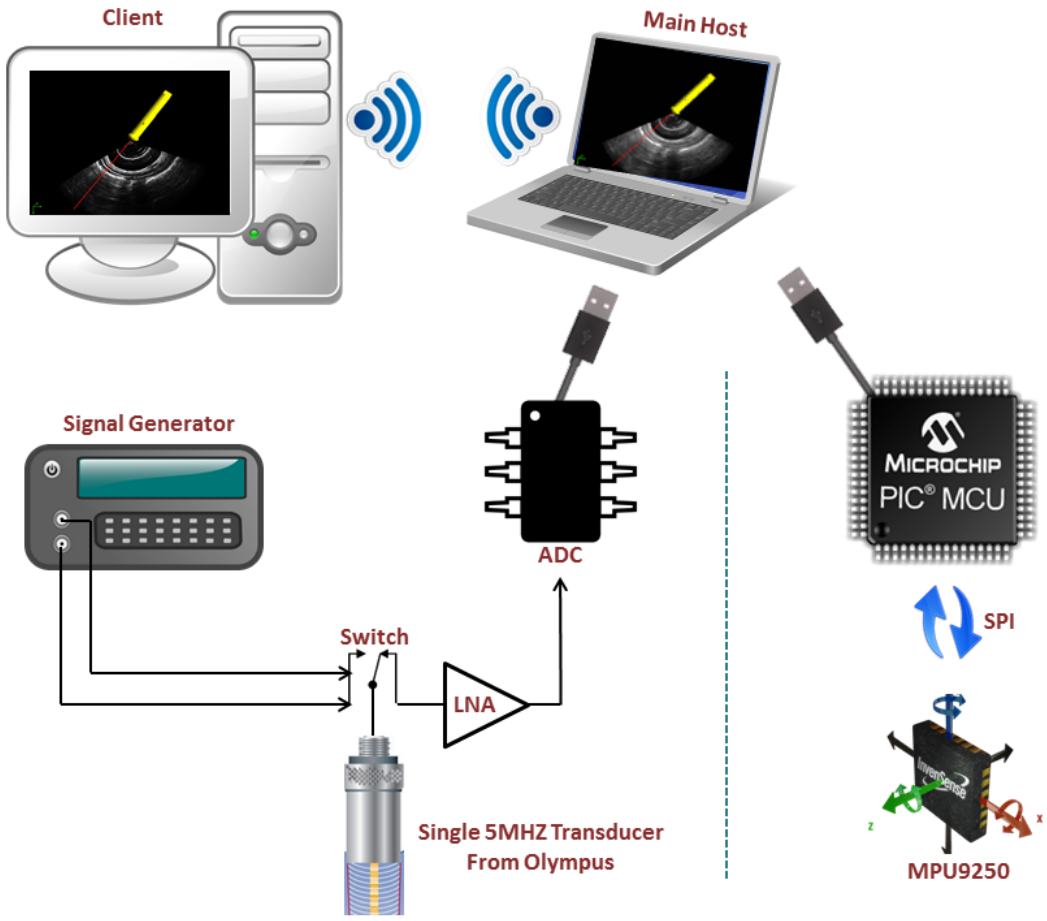

Figure 28: Diagram of first set-up

The figure demonstrates diagram of first set-up unit with WiFi connection between pc and laptop and single 5 MHz transducer. We used external arbitrary signal generator for drive and controlling the switch and etc.

Figure 29 demonstrates some essential parts of first set-up unit. Switch, Amplifier and Low pass filter are from mini-circuit while 5 MHz single transducer is from Olympus. Transducer is fixed to the bread board where MPU9250 and Mini32 is constructed on it too. This ables us to track position of the single transducer in 3D.

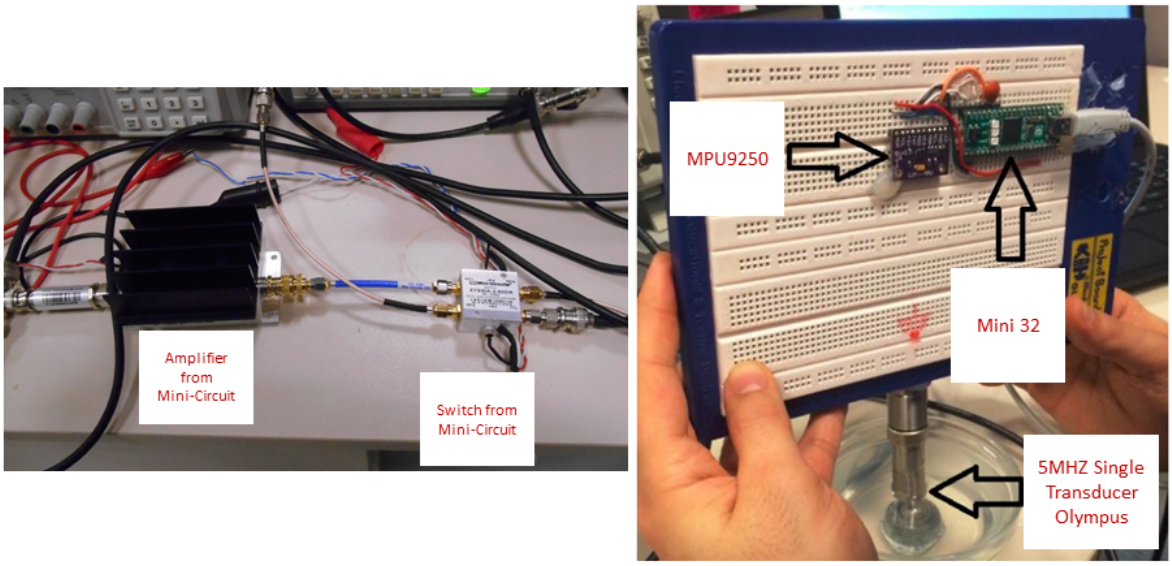

Figure 29: Some parts of first set-up unit

The figure demonstrates some essential parts of the first set-up unit.

As mentioned before final probe should have wireless interfaces to transfer data. therefore a laptop acts as host processor for our first set-up unit, and transfers data trough built in WiFi module to USB WiFi dongle that is connected to Stationary PC. Data are transmitted to PC while operator does ultrasound imaging as figure 30 is illustrated.

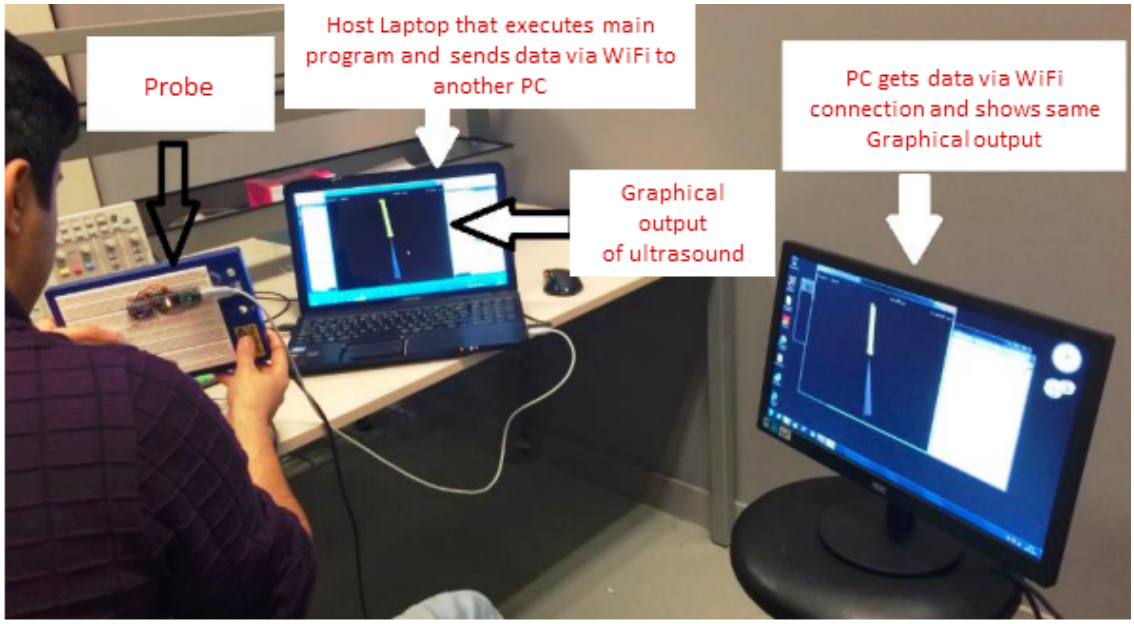

Figure 30: WiFi connection of first set-up unit

The figure demonstrates same graphical output on the PC that data were sent through WiFi connection. There was very low latency between Laptop and PC with low packet lost.

For testing result that can be achieved by using this set-up; we put two rigid cylinders inside a water container that was full of water. We used water as medium and impedance matching environment that roughly has same acoustic properties as human tissues. To avoid linear movement (translation) of the the probe and getting good result we attached probe from transducer side to a rotation stage. This tool gave us just rotation movement that used for ultrasound imaging of two rigid cylinders.

Probe was rotated for one time and gotten image is recorded on the Laptop screen as figure 31 illustrates. Obviously there is three bright lines in gotten image that are related to the top of the two cylinders and middle of them. For this set-up unit we used only one single transducer, by increasing transducer counts and using annular transducer best resolution of image can be gained.

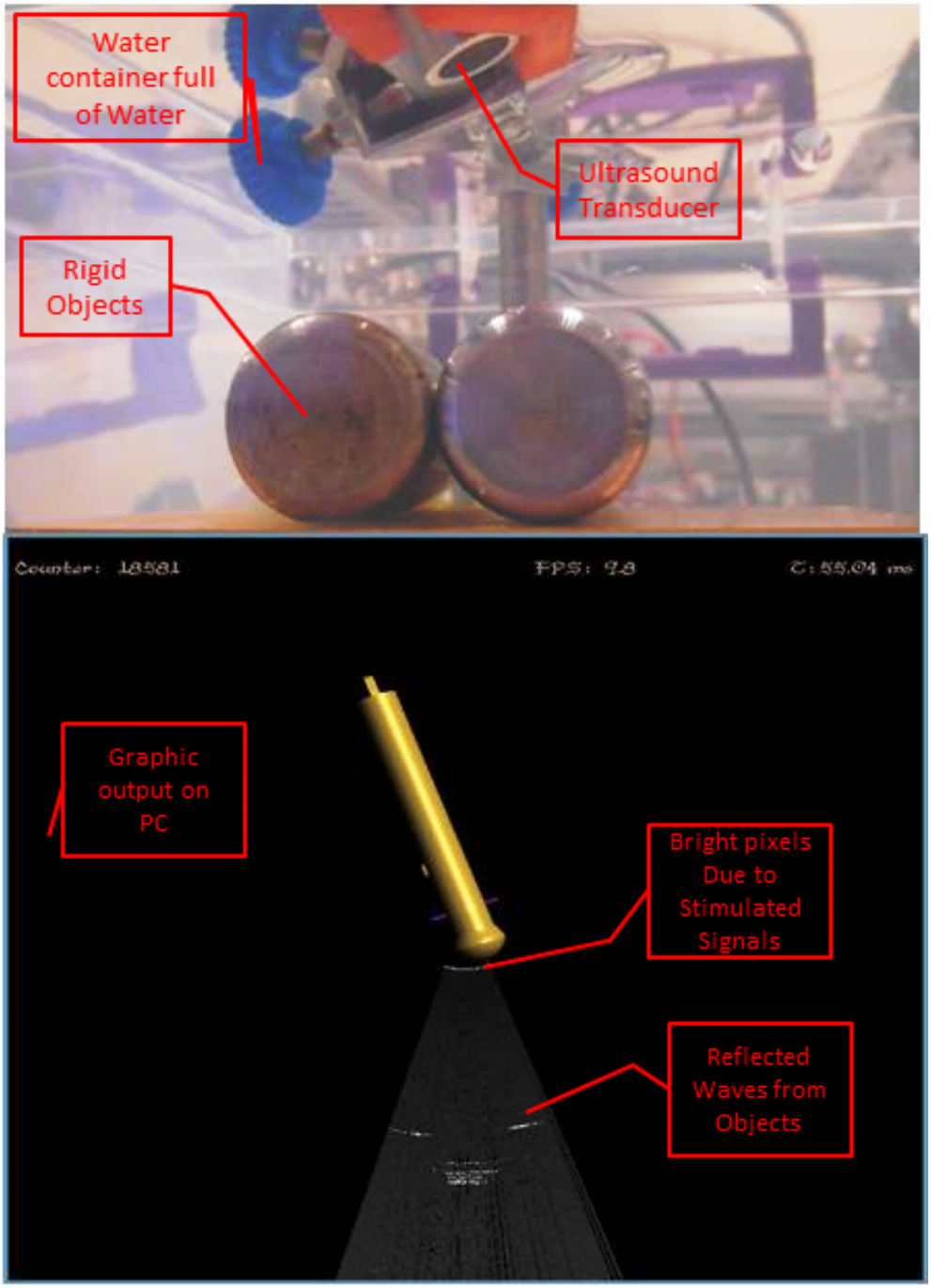

Figure 31: Ultrasound image gotten from first set-up unit

The figure demonstrates reflections from top and middle of the rigid cylinders sunken in water.

3.11 Second set-up unit with an Annular transducer

For miniaturization of the total system and fit it inside a hand held probe, we should design all driving and electronic parts on a single board, to gain that we designed switching and high voltage pulser on a single board as well as most rest of the system's parts. Also for getting good resolution and have more control on focal point of the ultrasound beams, we used an Annular transducer with four elements as illustrated in figure 32. We bought such annular transducers that have operation frequency around 5 MHz. Using Annular transducer has some advantages as mostly are mentioned before such as focal length changeability and so forth. Each element of the Annular transducer can be stimulated separately as well.

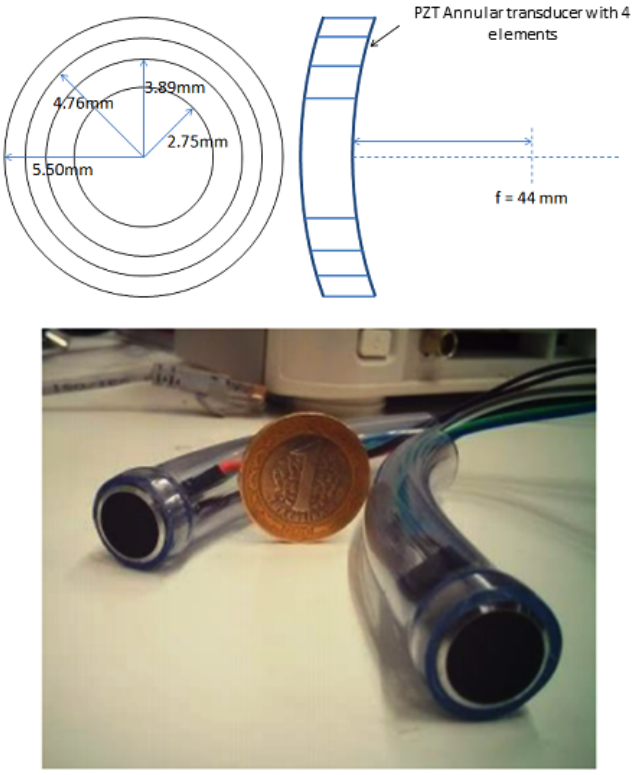

Figure 32: PZT Annular transducer with 4 elements

The figure demonstrates PZT Annular transducers that have 4 elements. This transducer is used for second set-up measurement unit.

An electronic board is designed for driving this Annular transducer as figure 33 shows. Stellaris Launchpad used for controlling the high voltage switch and high voltage pulser as well as sending PWM to TGC amplifier. The MCU first sends serial data to switch to close all channels switches except channel one which is connected to middle element of the Annular transducer. Then trigs the high voltage pulser to stimulate middle element. After stimulating the transducer, MCU sends another serial data to switch IC to close input line of the middle element and addresses the all elements outputs to four input of the AD8355 TGC amplifier (from analog deice).

AD8355 amplifies the signal with amplification ratio that MCU changes during the time. As mentioned before TGC amplifier has ability to change gain by applying proper voltage to it, therefor PWM outputs of the MCU are passed through a LPF to get suitable analog voltage, then these voltages are applied to AD8355 amplifier that inherently has 4 built in TGC amplifiers. 4 outputs of these signals are summed with a active circuit and guides the final output signal to ADC board that is introduced before.

We did not stimulate each element of the Annular transducer separately in this measurement set-up but we will do it. Also an Envelope detector will be added to output of the summing circuit to use advantages of that as before mentioned. To avoid getting more noise and having good earth connection, all boards are fitted on a copper board that is connected to earth (0V). Figure 34 illustrates all necessary boards of the second set-up unit on a copper board.

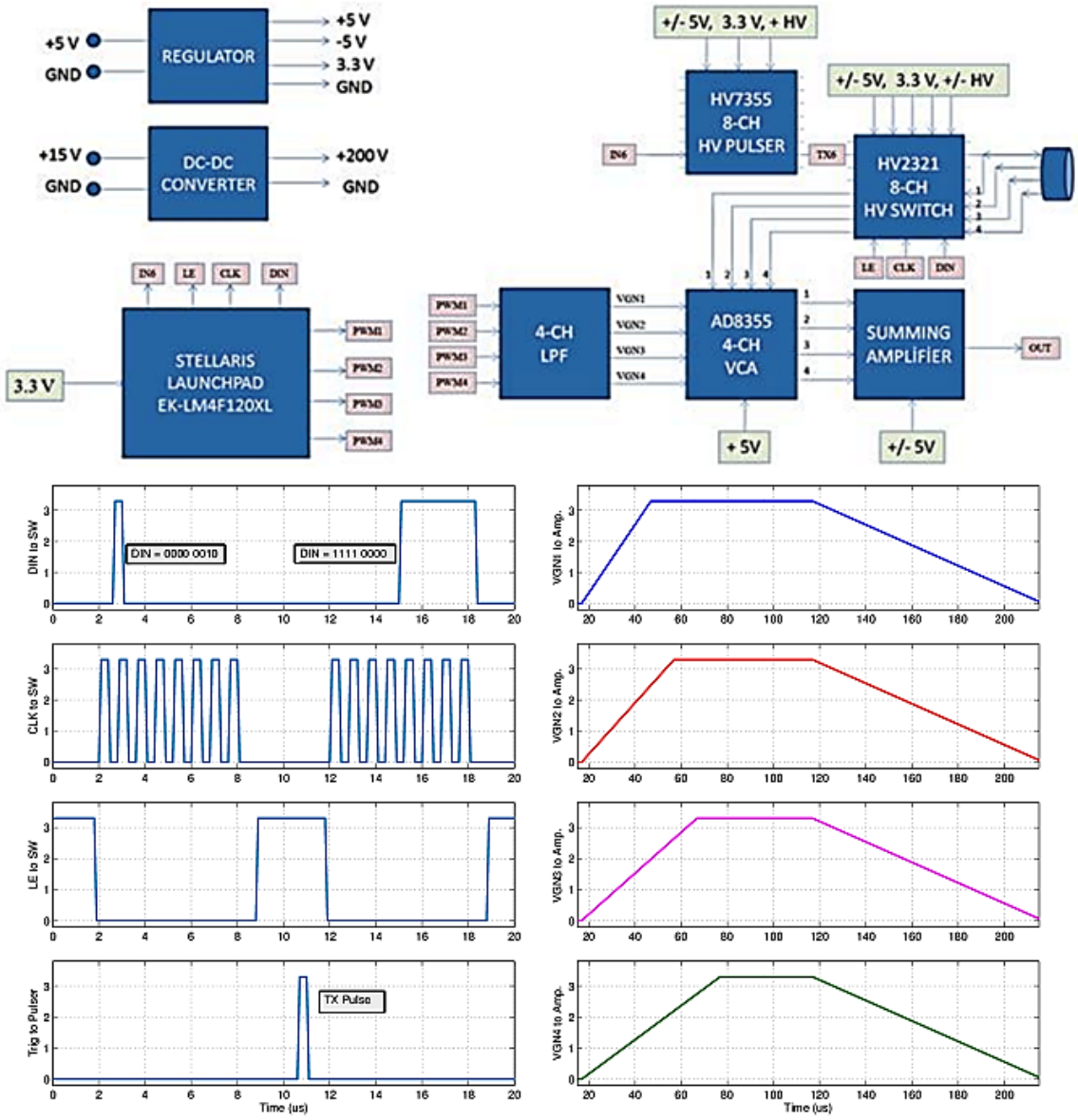

Figure 33: Diagram of pulser and switch board for second set-up unit

The figure demonstrates diagram of the pulser and switch board for second set-up unit that is designed at TOBB university. digital and analog voltages for controlling the board is shown here too.

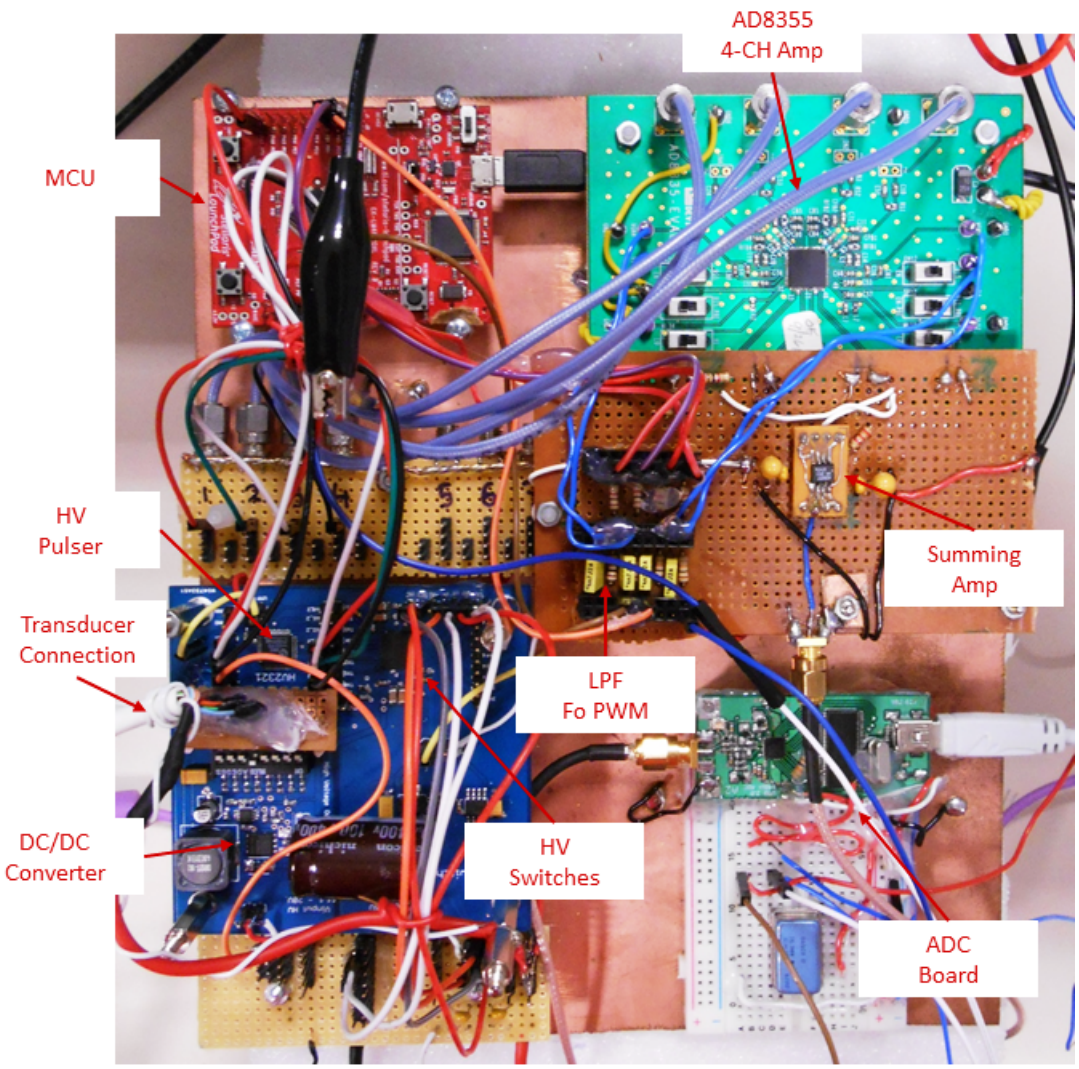

Figure 34: Electronic board of the second set-up unit on copper plate

The figure demonstrates most electronic parts of the second set-up unit on a copper plate. Copper plate is used to avoid boards to get noises from environments while it is connected to ground. The board needs +5v, -100V, +15v and GND for biasing and two USB connections to Stellaris Launchpad and ADC board. Later we will fit all these discrete electrical boards on a single tiny board that should be fitted in a small hand held probe.

Instead of using the large bread board that we had used in first set-up unit; This time we used small bread board and same Mini32 and MPU9250 as 3D position tracking unit where an Annular transducer is connected to that. Figure 35 shows the

probe.

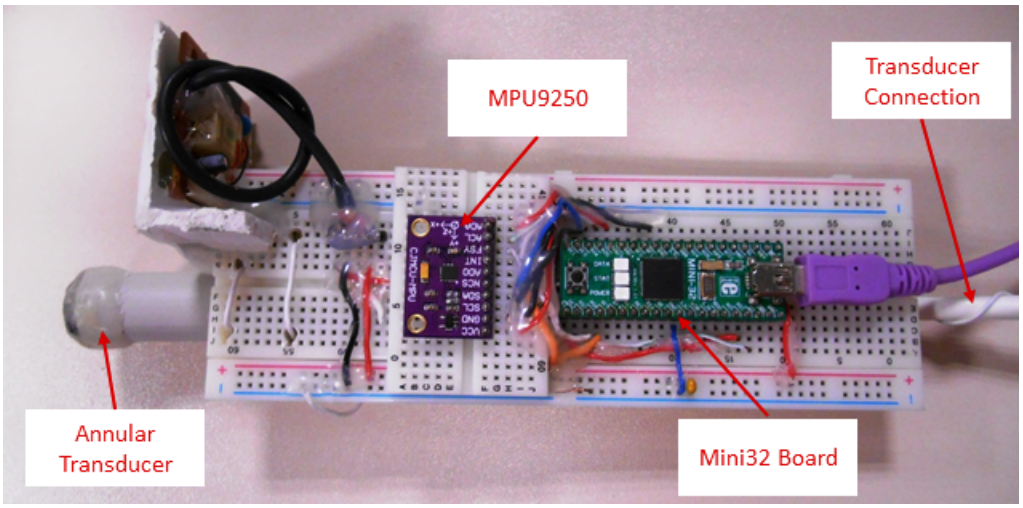

Figure 35: Probe of the second set-up unit

The figure demonstrates Mini32, MPU9250 boards as well as Annular transducer that are fixed on a breadboard.

For getting ultrasound images we used some different object and materials. Firstly we drilled some holes on two sides of water container symmetrically, then we put phantom wires in them. These phantom wires act as vessels inside organs. Finally we put this water container inside an another large water container full of water and did ultrasound imaging. Figure 36 shows whole the system, we will gather all these electronic parts inside a small probe.

Figure 37 shows how we drilled holes and passed phantom wires to water container. Figure 38, 39 illustrate the results that are gained from these phantom wires sunken inside the water and figure 40 shows phantom wires sunken inside a Gelatin.

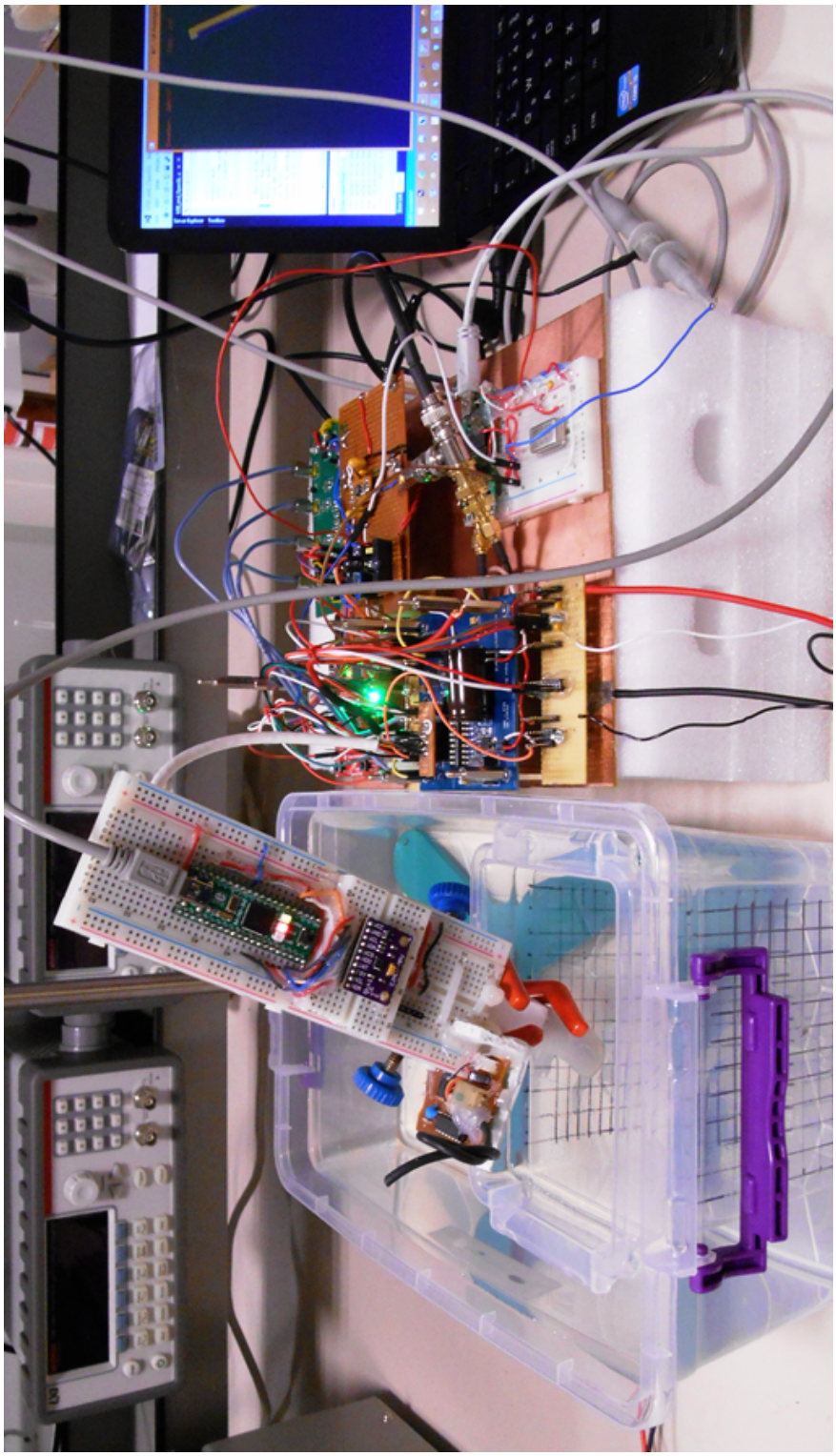

Figure 36: Final System that used for imaging

The figure demonstrates whole second set-up unit.

3.12 Results

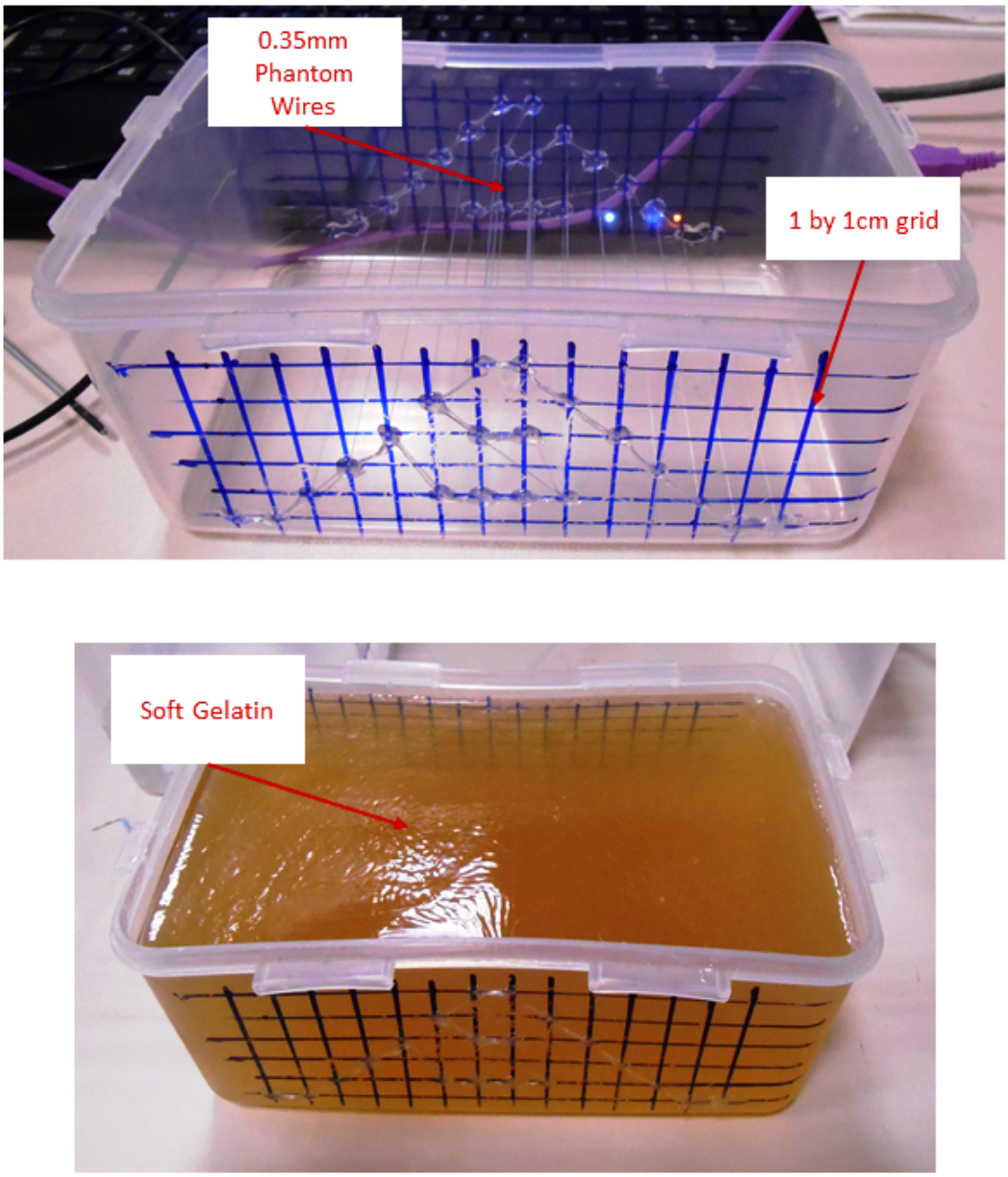

Figure 37: Water container and Gelatin

The figure demonstrates Water container before and after filling with gelatin and sunken phantom wires.

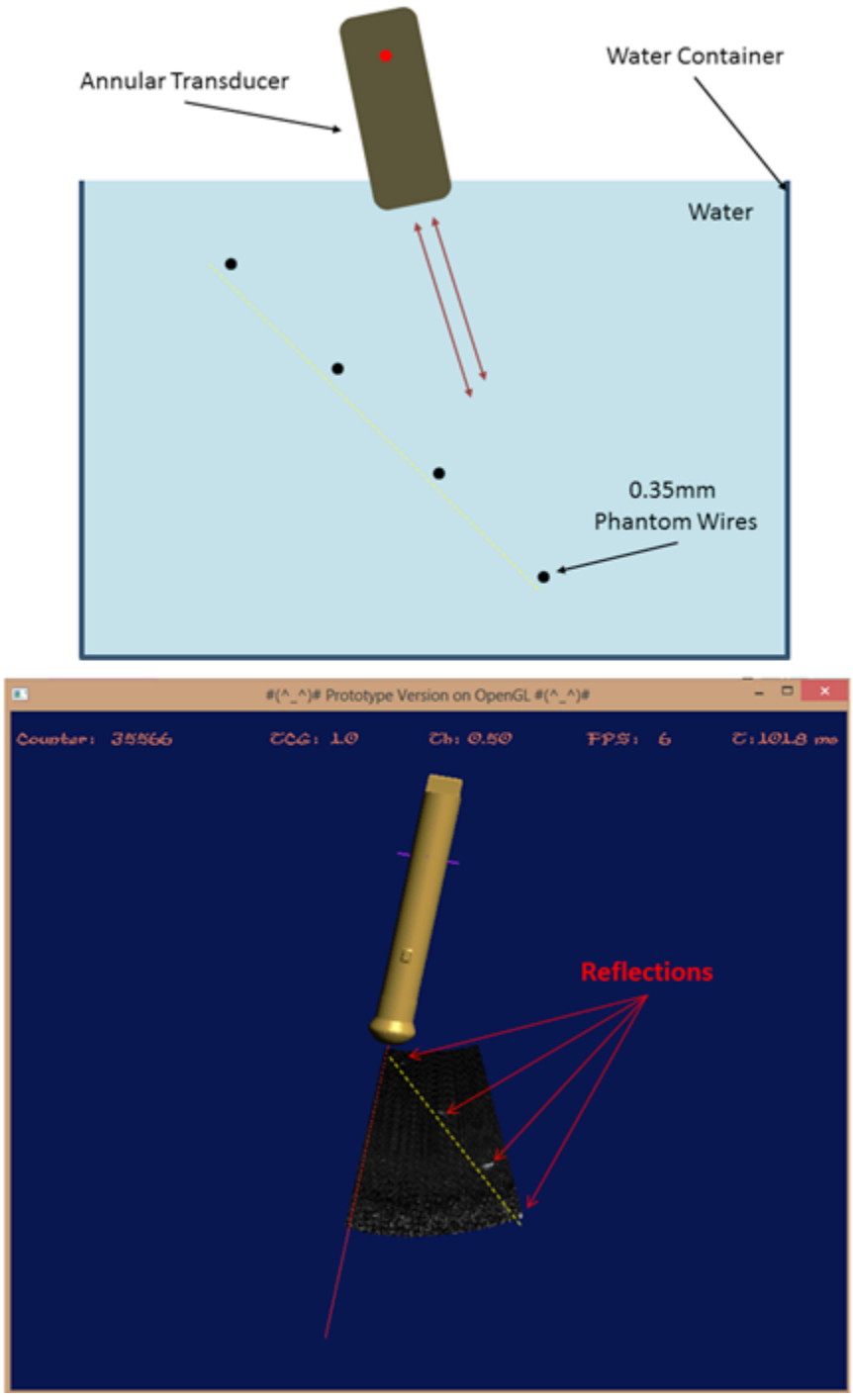

Figure 38: Ultrasound of Phantom wires sunken in water 1

The figure demonstrates an ultrasound image of 0.35 mm phantom wires sunken in water.

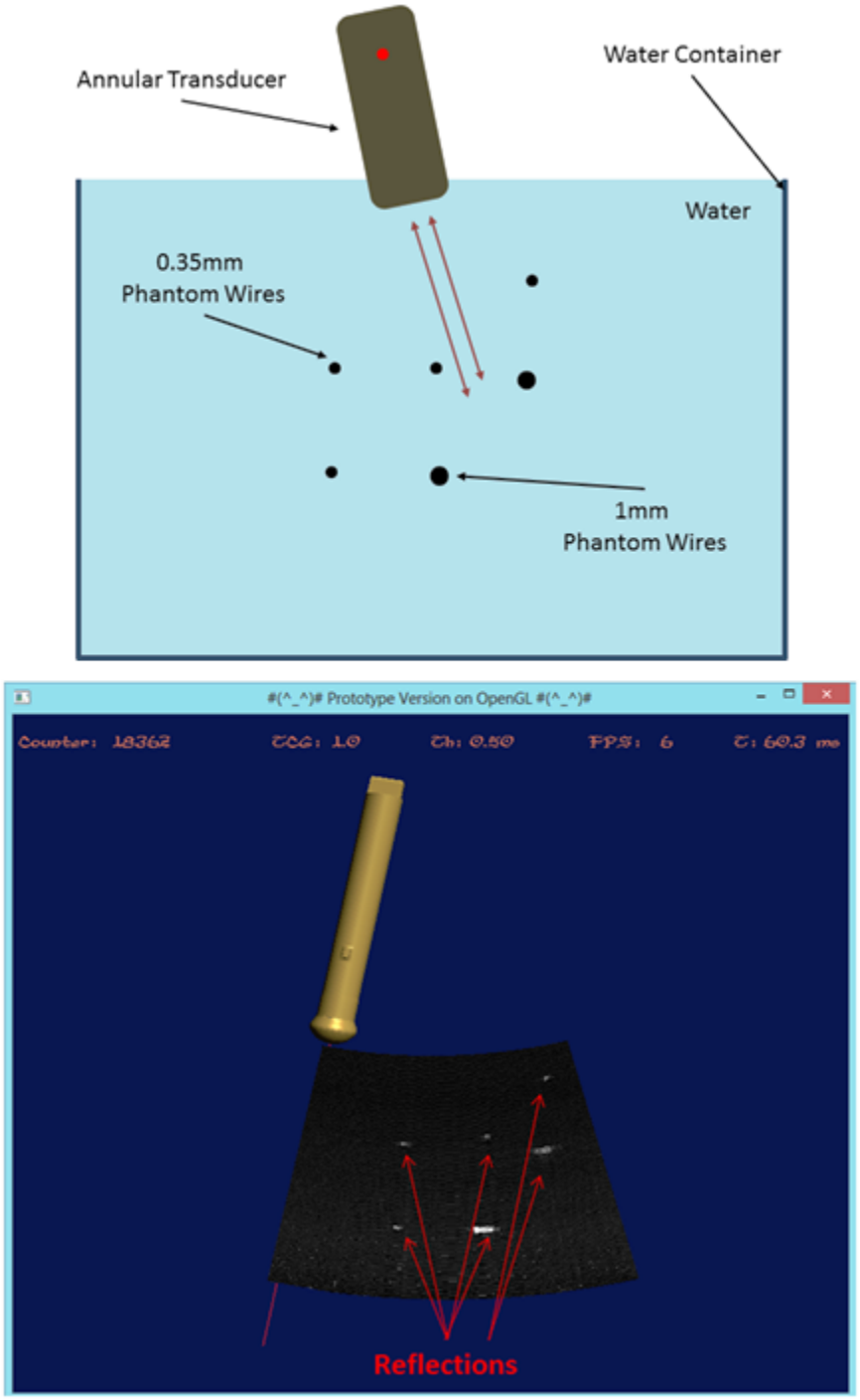

Figure 39: Ultrasound of Phantom wires sunken in water 2

The figure demonstrates an ultrasound image of 1 and 0.35 mm phantom wires sunken in water.

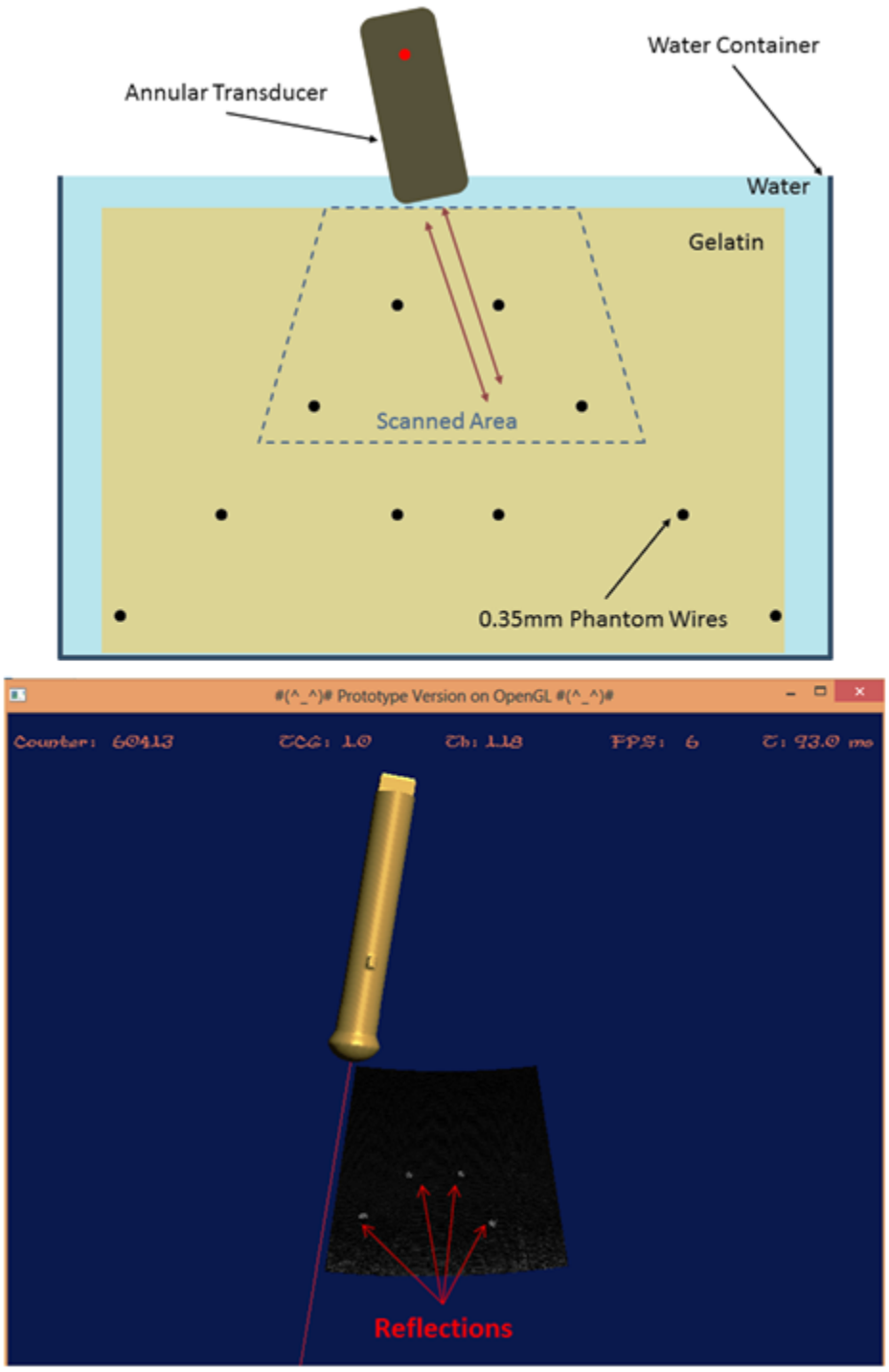

Figure 40: Ultrasound of Phantom wires sunken in gelatin

The figure demonstrates an ultrasound image of 0.35 mm phantom wires inside a Gelatin that is sunken in water.

CHAPTER IV

CONCLUSION

The prototype measurement set-up showed the idea works well. Next step for this project is designing an annular transducer based on CMUT that is mentioned before. The annular transducer based on CMUT will be replaced with currently used transducer. Because low power consumption is desired, then we may use new module based on motion processor instead of MPU9250, such as MM7150. This module will give us quaternion directly without executing our QUEST algorithm. Electrical driving units all will be fitted on a small board, which gives the system independency to external driving units. A Linux based microprocessor that has built in OpenGL, will operate as brain of the probe; it will get both data from sensors and ultrasound data as well as executing all the algorithms inside.

Because desired version is fully portable so it should have wireless communication. Linux based microprocessor has ability to use WiFi USB module without more complexity. Processed data will be transmitted via WiFi module to Laptop, Tablet or smart phone. All the mentioned components and units are checked separately without any problem. Currently we are gathering all units inside a hand held probe which will have several advantages such as, adjustable focal length for annular transducer, independency to any external devices, has ability to transmit data to desired destination wirelessly (up to 25 Mbit per second) for either raw data or just gotten images, fully 3D motion tracking ability which gives operator fully freedom during the scanning (6 DOF) and etc.

The cost of this system is proposed to be around 1000 dollars that it is very cheap in compare to other commercial portable brands. Finally since the probe is portable,

it can be used in ambulances in emergency cases where there are internal injuries or in clinics for routine pre examination and checkups. It will able doctors to use this portable ultrasound system frequently in their routine checkups like stethoscope.

APPENDIX A

QUEST CODE

```
1
2 void QUEST_KALMAN(void)
3 {
4   float norm_Accel_Sensor_In_Filtered, norm_compass,
      norm_gyro, norm_q, xmag, ymag, zmag, q[4], q_final[4],
      e_m[4], q_g[4], q_r[4], q_p[4], q_y[4], q_r_r[4],
      q_p_r[4], b_m[4], in[4], in1[4], in2[4], M[2], N[2],
      Reverse[4], Result[4], Result1[4];
5   float Sin_Pitch, Cos_Pitch, Sin_Half_Pitch,
      Cos_Half_Pitch, Sin_Roll, Cos_Roll, Sin_Half_Roll,
      Cos_Half_Roll, Sin_Yaw, Cos_Yaw, Sin_Half_Yaw,
      Cos_Half_Yaw, Accel_Sensor_In_Filtered_offset[4],
      b_m_offset[4], q_a[4], q_a_r[4], e = 0.1, alfa = 20 *
      (M_PI / 180), Roll, Pitch, Yaw;
6   float Accel_Sensor_In_Filtered[4], R[3][3];
7   int j, s, flag = 0, k;
8
9   for (j = 0; j < 4; j++)
10    Accel_Sensor_In_Filtered[j] = Accel_Sensor_Filtered[j];
11
12
```

```
13  norm_Accel_Sensor_In_Filtered =
        sqrt(pow(Accel_Sensor_In_Filtered[1], 2) +
        pow(Accel_Sensor_In_Filtered[2], 2) +
        pow(Accel_Sensor_In_Filtered[3], 2));
14  norm_compass = sqrt(pow(compass[1], 2) + pow(compass[2],
        2) + pow(compass[3], 2));
15
16  for (j = 0; j < 4; j++)
17    compass[j] = compass[j] / norm_compass;
18
19  for (j = 0; j < 4; j++)
20    b_m[j] = compass[j];
21
22  Sin_Pitch = Accel_Sensor_In_Filtered[1] /
        norm_Accel_Sensor_In_Filtered;
23  Cos_Pitch = sqrt(1 - pow(Sin_Pitch, 2));
24
25  if (Cos_Pitch <= e)
26  {
27    q_a[0] = cos(alfa / 2);
28    q_a[1] = q_a[3] = 0;
29    q_a[2] = sin(alfa / 2);
30
31    Quat_Reverse(q_a, q_a_r);
32
33    Quat_Multiply(q_a, Accel_Sensor_In_Filtered, Result);
34
```

```
35      Quat_Multiply(Result, q_a_r,
            Accel_Sensor_In_Filtered_offset);
36
37      for (j = 0; j < 4; j++)
38        Accel_Sensor_In_Filtered[j] =
              Accel_Sensor_In_Filtered_offset[j];
39
40      Quat_Multiply(q_a, compass, Result);
41
42      Quat_Multiply(Result, q_a_r, b_m_offset);
43
44      for (j = 0; j < 4; j++)
45        b_m[j] = b_m_offset[j];
46
47      norm_Accel_Sensor_In_Filtered =
            sqrt(pow(Accel_Sensor_In_Filtered[1], 2) +
            pow(Accel_Sensor_In_Filtered[2], 2) +
            pow(Accel_Sensor_In_Filtered[3], 2));
48
49      Sin_Pitch = Accel_Sensor_In_Filtered[1] /
            norm_Accel_Sensor_In_Filtered;
50      Cos_Pitch = sqrt(1 - pow(Sin_Pitch, 2));
51      flag = 1;
52    }
53
54    if (Sin_Pitch < 0)
55      s = -1;
```

```
56  else
57    s = 1;
58  Sin_Half_Pitch = s * sqrt((1 - Cos_Pitch) / 2);
59  Cos_Half_Pitch = sqrt((1 + Cos_Pitch) / 2);
60
61  Sin_Roll = -Accel_Sensor_In_Filtered[2] /
      (norm_Accel_Sensor_In_Filtered * Cos_Pitch);
62  Cos_Roll = -Accel_Sensor_In_Filtered[3] /
      (norm_Accel_Sensor_In_Filtered * Cos_Pitch);
63
64  if (Sin_Roll > 1)
65    Sin_Roll = 1;
66  if (Sin_Roll < -1)
67    Sin_Roll = -1;
68  if (Cos_Roll > 1)
69    Cos_Roll = 1;
70  if (Cos_Roll < -1)
71    Cos_Roll = -1;
72
73  if (Sin_Roll < 0)
74    s = -1;
75  else
76    s = 1;
77  Sin_Half_Roll = s * sqrt((1 - Cos_Roll) / 2);
78  Cos_Half_Roll = sqrt((1 + Cos_Roll) / 2);
79
80
```

```
81   q_p[0] = Cos_Half_Pitch;
82   q_p[1] = q_p[3] = 0;
83   q_p[2] = Sin_Half_Pitch;
84
85   q_r[0] = Cos_Half_Roll;
86   q_r[2] = q_r[3] = 0;
87   q_r[1] = Sin_Half_Roll;
88
89   Quat_Reverse(q_p, q_p_r);
90   Quat_Reverse(q_r, q_r_r);
91   Quat_Multiply(q_p, q_r, Result);
92   Quat_Multiply(Result, b_m, Result1);
93   Quat_Multiply(Result1, q_r_r, Result);
94   Quat_Multiply(Result, q_p_r, e_m);
95
96   N[0] = -0.28735;            // I got them practically
97   N[1] = -0.95783;           //
98   M[0] = e_m[1] / sqrt(pow(e_m[1], 2) + pow(e_m[2], 2));
99   M[1] = e_m[2] / sqrt(pow(e_m[1], 2) + pow(e_m[2], 2));
100
101  Sin_Yaw = (-M[1] * N[0]) + (M[0] * N[1]);
102  Cos_Yaw = (M[0] * N[0]) + (M[1] * N[1]);
103
104  if (Sin_Yaw > 1)
105    Sin_Yaw = 1;
106  if (Sin_Yaw < -1)
107    Sin_Yaw = -1;
```

```
108   if (Cos_Yaw > 1)
109     Cos_Yaw = 1;
110   if (Cos_Yaw < -1)
111     Cos_Yaw = -1;
112
113   if (Sin_Yaw < 0)
114     s = -1;
115   else
116     s = 1;
117   Sin_Half_Yaw = s * sqrt((1 - Cos_Yaw) / 2);
118   Cos_Half_Yaw = sqrt((1 + Cos_Yaw) / 2);
119
120   q_y[0] = Cos_Half_Yaw;
121   q_y[1] = q_y[2] = 0;
122   q_y[3] = Sin_Half_Yaw;
123
124   Quat_Multiply(q_y, q_p, Result);
125   Quat_Multiply(Result, q_r, q);
126   norm_q = sqrt(pow(q[0], 2) + pow(q[1], 2) + pow(q[2], 2) +
        pow(q[3], 2));
127   for (j = 0; j < 4; j++)
128     q[j] = q[j] / norm_q;
129
130   if (flag == 1)
131   {
132     Quat_Multiply(q, q_a, Result);
133
```

```
134     for (j = 0; j < 4; j++)
135       q[j] = Result[j];
136
137     flag = 0;
138     norm_q = sqrt(pow(q[0], 2) + pow(q[1], 2) + pow(q[2], 2)
          + pow(q[3], 2));
139     for (j = 0; j < 4; j++)
140       q[j] = q[j] / norm_q;
141   }
142
143   u_Quest[0] = (float)2 * acos(q[0]);
144   u_Quest[1] = (float)q[1] / sin(u_Quest[0] / 2);
145   u_Quest[2] = (float)q[2] / sin(u_Quest[0] / 2);
146   u_Quest[3] = (float)q[3] / sin(u_Quest[0] / 2);
147   u_Quest[0] = (float)(u_Quest[0] / M_PI) * 180;
148
149   for (j = 25; j < 29; j++)
150     Array_3D_Position[counter - 1][j] = u_Quest[j - 25];
```

[1] Bartlett, Stewart Gavin, and Paul James Hirschausen. "Apparatus and method for medical scanning." U.S. Patent Application 12/675,473.

[2] Baran, Jonathan M. "Design of Low-Cost Portable Ultrasound Systems." Biomedical Engineering, University of Wisconsin-Madison (2008).

[3] Berman, Michael, et al. "3-dimensional ultrasonic imaging." U.S. Patent No. 6,315,724. 13 Nov. 2001.

[4] Hopkins, Andrew David. "Ultrasound probe with accelerometer." U.S. Patent No. 8,914,245. 16 Dec. 2014.

[5] Hetz, Walter, and Richard Soldner. "Ultrasonic apparatus for medical diagnosis." U.S. Patent No. 4,110,723. 29 Aug. 1978.

[6] CN 202211705 U

[7] Patent 2008-229245 (P2008-229245A)

[8] Sato, Tomoo. "Ultrasound diagnostic apparatus and ultrasound image producing method." U.S. Patent Application 13/469,808.

[9] Kimoto, Takashi, et al. "Ultrasound diagnostic apparatus and ultrasound diagnostic system." U.S. Patent Application 13/636,835.

[10] Bayram, Baris, et al. "Capacitive micromachined ultrasonic transducer design for high power transmission." Ultrasonics, Ferroelectrics, and Frequency Control, IEEE Transactions on 52.2 (2005): 326-339.

[11] Ladabaum, Igal, et al. "Surface micromachined capacitive ultrasonic transducers." Ultrasonics, Ferroelectrics, and Frequency Control, IEEE Transactions on 45.3 (1998): 678-690.

[12] Bleser, Gabriele, and Didier Stricker. "Advanced tracking through efficient image processing and visual inertial sensor fusion." Computers and Graphics 33.1 (2009): 59-72.

[13] Armesto, Leopoldo, Josep Tornero, and Markus Vincze. "Fast ego-motion estimation with multi-rate fusion of inertial and vision." The International Journal of Robotics Research 26.6 (2007): 577-589.

[14] Corke, Peter, Jorge Lobo, and Jorge Dias. "An introduction to inertial and visual sensing." The International Journal of Robotics Research 26.6 (2007): 519-535.

[15] Yun, Xiaoping, Eric R. Bachmann, and Robert B. McGhee. "A simplified quaternion-based algorithm for orientation estimation from earth gravity and magnetic field measurements." Instrumentation and Measurement, IEEE Transactions on 57.3 (2008): 638-650.

[16] Luinge, Hendrik Johannes. Inertial sensing of human movement. Twente University Press, 2002.

[17] McGhee, Robert B. "The factored quaternion algorithm for orientation estimation from measured Earth gravity and magnetic field." MOVES Inst., Naval Postgraduate School, Monterey, CA (2004).

[18] Yun, Xiaoping, and Eric R. Bachmann. "Design, implementation, and experimental results of a quaternion-based Kalman filter for human body motion tracking." Robotics, IEEE Transactions on 22.6 (2006): 1216-1227.

VITA

Mohammad Rahim Sobhani was born in Tabriz, Iran, in 1989. He received the B.Sc. in Electrical and Eletronics Engineering - Biomedical Engineering (Bioelectric) with CGPA of 3.71/4 (first rank among his classmates) from Sahand University of Technology, Tabriz, Iran, in 2012. Currently he is M.Sc. candidate in Electrical and Electronics engineering at ÖZYEĞİN University, Istanbul, Turkey. His research interests include, analog circuit design, MEMS and opto-MEMS applications in medicine, ultrasound imaging, signal and image processing.

He got acceptance from same university (ÖZYEĞİN university) for Ph.D. program in Electrical and Electronics Engineering with full scholarship and financial support. He will start his Ph.D. since sept 2015, under supervision of Assoc. Prof. G. Göksenin Yaralıoğlu as well as being TA and RA in the university for electrical and electronics engineering department.

Some portions of this dissertation was accepted in 14th international workshop on Micromachined Ultrasound Transducers, 19th of may 2015, Dresden, Germany.